PROCESSING SOLAR PROBE TRACKING DATA

(Sunblazer)

by

Harry T. Doerer
Robert W. Langley

CSR T-66-5 August 1966

PROCESSING SOLAR PROBE TRACKING DATA

by

Harry T. Doerer
Robert W. Langley

Submitted to the Department of Aeronautics and Astronautics on 22 August 1966, in partial fulfillment of the requirements for the degree of Master of Science.

ABSTRACT

The Sunblazer is a small solar probe that must be tracked by measuring azimuth, elevation, and range rate at one station on the Earth's surface. The geometrical aspects of relating Earth station coordinates to an inertial coordinate system are examined. A Kalman filter is developed to provide a recursive maximum-likelihood estimate of the deviation of the probe's true state from a nominal state. The filter is incorporated in the flow chart of a complete data processing program. The diagonal elements of the state deviation error covariance matrix at conjunction are computed for varying qualities of range rate data and are shown to coincide with the results of a similar investigation performed by D. O. Madl. In addition, the possibility of optimally scheduling the measurements is discussed.

Thesis Supervisor: John V. Harrington

Title: Professor of Aeronautics and Astronautics; and Director, Center for Space Research

ACKNOWLEDGEMENTS

The authors wish to express their appreciation to their thesis advisor, Professor John V. Harrington for his direction, Lt. Dennis Madl for initially suggesting the problem, Mr. William T. MacDonald, Mr. John H. Fagan, and other staff members of the Experimental Astronomy Laboratory and the Center for Space Research for their advice and encouragement, and Miss Linda Morrissey for typing this thesis.

Acknowledgement is made to the Department of the Air Force and the Air Force Institute of Technology for making this work possible.

Acknowledgement is also made to the Department of Civil Engineering at MIT for the use of their IBM System 360.

TABLE OF CONTENTS

TABLE OF CONTENTS(continued)

TABLE OF CONTENTS(continued)

SYMBOLS

$( )_o$	Initial value of ( )
$( )_i$	Value of ( ) at stage i
$( )_N$	The quantity ( ) is nominal.
$(\underline{\ })$	Quantity ( ) is a column vector.
$(\bar{\ })$	Estimated value of ( ) before measurements
$(\hat{\ })$	Best estimate of ( )
$\delta( )$	Deviation of ( ) from a nominal value
$(\dot{\ })$	Time derivative of ( )
$(\underline{\ })^{(n)}$	Vector $(\underline{\ })$ is coordinatized in frame n.
$( )^T$	The transpose of the matrix or column vector ( )
$( )^{-1}$	Inverse of the square matrix ( )
$E( )$	Expected value of ( )
$f( )$	A function of ( )
$\underline{\Phi}_i$	6x6 state transition matrix from stage i to i+1
M	6x6 error covariance matrix before measurement
P	6x6 error covariance matrix of the best estimate of the state deviation
H	3x6 matrix relating measurement deviations to state deviations
K	6x3 filter weighting matrix
R	3x3 diagonal measurement error covariance matrix
C_j^k	3x3 orthogonal transformation matrix from coordinate frame j to coordinate frame k
$\underline{\rho}$	Position vector of the probe with respect to the tracking station

$\underline{R}_{ss}$	Position vector of the tracking station with respect to the Sun's center
$\underline{R}_{sb}, \underline{V}_{sb}$	Position and velocity vectors of the Earth-Moon barycenter with respect to the Sun's center
$\underline{R}_{eb}, \underline{V}_{eb}$	Position and velocity vectors of the Earth-Moon barycenter with respect to the Earth's center
$\underline{R}_{em}, \underline{V}_{em}$	Position and velocity vectors of the Moon with respect to the Earth's center
$\underline{R}, \underline{V}$	Position and velocity vectors of the probe with respect to the Sun's center
$\underline{r}$	Position of the tracking station with respect to the Earth's center
$\underline{x}$	6 component state vector consisting of $\underline{R}$ and $\underline{V}$
$\underline{e}$	Difference between true state deviation and estimated state deviation
$\underline{a}^T$	A 3 component row vector that represents the first three elements in the first row of the H matrix coordinatized in frame 5
$\underline{b}^T$	A 3 component row vector that represents the first three elements in the second row of the H matrix coordinatized in frame 5
$\underline{c}^T$	A 6 component row vector that represents the third row of the H matrix in frame 5
$\underline{h}_1^T$, $\underline{h}_2^T$	$\underline{a}^T$ and $\underline{b}^T$ respectively coordinatized in frame 6
$\underline{h}_3^T$	$\underline{c}^T$ coordinatized in frame 6
r	Magnitude of $\underline{r}$
ρ	Magnitude of $\underline{\rho}$
A	Azimuth angle
L	Elevation angle
$\dot{\rho}$	The projection of $\dot{\underline{\rho}}$ along $\underline{\rho}$
m	A measurement
m_e	Mass of the Earth
m_m	Mass of the Moon
η	Relates $\underline{R}_{em}$ to $\underline{R}_{eb}$ and $\underline{V}_{em}$ to $\underline{V}_{eb}$

σ_{jk}	Standard deviation of j in the k direction
ϵ	Obliquity
$\bar{\epsilon}$	Mean obliquity
$\delta\epsilon$	Nutation of the equator in obliquity
$\delta\psi$	Nutation of the equator in longitude
γ (T)	Greenwich hour angle
γ_m(T)	Mean Greenwich hour angle
$\delta\alpha$	Difference between the true and the mean Greenwich hour angle
ϕ	Geocentric latitude
ℓ	Longitude
ω	Rate of rotation of the Earth about its polar axis
JD	Julian date
UT	Universal Time
ET	Ephemeris Time
ΔT	Correction factor to relate ET to UT

NUMERICAL VALUES

η	1.0/82.3015
$\bar{\epsilon}$	23.4457587°
π	3.141593
μ_{sun}	4.6868171×10^{21} ft^3/sec^2 (Ref. 12)
1 AU	149.599×10^6 Km
1 Earth Radius	6378.3255 Km
1 Besselian Century	100 Yr = 36525 days
1 Time Unit (TU)	1 Yr
1 Radian	57.29577957°

TRACKING STATION COORDINATES (El Campo, Texas)

ϕ	28.84°N
ℓ	96.25°W = 263.75°
r	4260.3278×10^{-8} AU

CHAPTER 1

INTRODUCTION

The Sunblazer solar probe is to be launched from Wallops Island in the summer of 1968. It will be the first in a proposed series of solar satellites which will be used to investigate properties of the Sun's corona. The MIT Center for Space Research has published a complete summary of the objectives of the project and the composition of the probe itself in Report PR-5255-5.

1.1 General Problem

This thesis is concerned with the tracking of this probe in a manner which will utilize Kalman filtering techniques to obtain a best estimate of its position and velocity. The probe will contain a radio transmitter which will transmit at two predesignated frequencies during the entire mission. Directional antennas at the El Campo, Texas, tracking station are to be used to obtain the azimuth and elevation angles of the probe during the flight. Knowing the transmitted frequencies, the Doppler shift of the received signal can be found. This Doppler shift is used to determine the range rate of the probe relative to the station. These three quantities, azimuth, elevation, and range rate, can

be used to determine the position and velocity of the spacecraft.

Two facts lead to the use of filtering techniques in the determination of vehicle position and velocity. First, azimuth, elevation, and range rate may be measured many times during the course of the vehicle's flight. Second, application of the laws of celestial mechanics will determine an approximation for the position and velocity of the spacecraft. The redundancy inherent in the information available allows the inaccuracies in the measuring system and the inaccuracies in the approximate solution to be partially filtered. How well these inaccuracies may be eliminated depends upon, among other factors, their magnitude, the number of measurements taken, and the times at which the measurements are taken.

1.2 The Objectives and the Order of Presentation

The first of the two main objectives of this thesis is the development of a computational procedure which uses actual data from the tracking station to compute a best estimate of the position and velocity of the probe. This procedure is described by a flow chart in Chapter 5 from which a computer program can be written to process actual measurement data. The second objective is to verify the results and conclusions presented by D. O. Madl in his Master's Thesis (Ref. 13). This was done by using a model, as exact as possible, of the Sun-Earth-probe system and computing what Madl called a "Figure of Merit." The comparison with Madl's results is

made in Chapter 6. Also included in this chapter are some comments concerning optimal scheduling of the measurements which are an outgrowth of the main study of the thesis.

Chapter 2 describes the coordinate frames and transformations incorporated in the mathematical description of the model. These coordinate transformations are used to compute the elements of a matrix which relates the state of the probe to the measurements. The analytic expressions in this matrix are derived in Chapter 3. This matrix is an important part of the filter which is used in the data processing program. Chapter 4 is devoted to the discussion and explanation of this filter. The program used to compute the numerical results presented in Chapter 6 is described and listed in the Appendix.

1.3 General Assumptions

Several assumptions are inherent in all the material presented. Range rate is obtained by the reception of radio signals from the probe as previously stated. It is assumed that pure range rate data are available; that is, all biases have been removed from the radio signal, and the Doppler problem has been solved to procure range rate. If the data contain unknown biases, the filter can be altered to obtain a best estimate of these biases, and they can be removed.

The nominal probe orbit used for the calculations of the "Figure of Merit" is that suggested by Harrington and used by Madl.

The characteristics of this orbit are as follows:

Perihelion radius	.528 AU
Aphelion radius	1.00 AU
Period	2/3 TU
Inclination to the ecliptic at time of injection	0°
Launch date	22 Jul 66

This orbit is a close approximation to the orbits intended for the actual flights.

CHAPTER 2

GEOMETRICAL ASPECTS OF TRACKING THE PROBE

In view of the goals of the Sunblazer project, it is imperative to know the state of the probe relative to the Sun. Since data received at the tracking station yield information concerning the probe state with respect to the station, it is natural to assume that the desired probe state can be calculated by determining the station position and velocity with respect to the Sun.

$$\underline{R} = \underline{\rho} + \underline{R}_{ss} \qquad (2.1)$$

$$\underline{V} = \dot{\underline{\rho}} + \underline{V}_{ss}$$

$\underline{R}$, $\underline{\rho}$, and $\underline{R}_{ss}$ are position vectors from Sun to probe, station to probe, and Sun to station, respectively, and equation 2.2 is the time derivative of 2.1. This, however, is not the case because $\underline{\rho}$ and $\dot{\underline{\rho}}$ cannot be determined with sufficient accuracy from the tracking data.

To obtain the desired accuracy in the calculation of $\underline{R}$ and $\underline{V}$, it is necessary to take a rather indirect approach in which nominal values are specified for the state. This permits nominal values to be calculated for $\underline{\rho}$ and $\dot{\underline{\rho}}$.

$$\underline{\rho}_N = \underline{R}_N - \underline{R}_{ss} \qquad (2.3)$$

$$\dot{\underline{\rho}}_N = \underline{V}_N - \underline{V}_{ss} \qquad (2.4)$$

Once nominal information is obtained, a Kalman filter can be used to estimate the probe's true state.

To determine the nominal values in equations 2.3 and 2.4, it is necessary to relate the vectors in a single coordinate frame. To do this, the complex motions of the Earth in inertial space must be examined, and several intermediate coordinate frames must be defined.

2.1 Motion of the Earth's Center

The center of the Earth revolves around the Earth-Moon barycenter in approximately an elliptic orbit with a period of about 28 days. The orbit of the Earth's center around the barycenter can be inferred from knowledge of the Moon's orbit around the Earth. It is this barycenter that is in a slightly perturbed elliptic orbit around the solar system barycenter, which, to a high degree of accuracy, is the center of the Sun. To aid in the following analysis, $\underline{R}_{ss}$ will be divided into three different position vectors, $\underline{R}_{eb}$, $\underline{R}_{sb}$, and $\underline{r}$, which are described in figure 2.1. From the illustration it can be seen that

$$\underline{\rho} = \underline{R} + \underline{R}_{eb} - \underline{R}_{sb} - \underline{r} \qquad (2.5)$$

2.2 Coordinate Frames

The selection of the coordinate frames illustrated in figure 2.1 was motivated by the availability of information concerning the orientations of these frames with respect to each other. The relationships between the frames are based on the time varying orientations of the Earth's equatorial

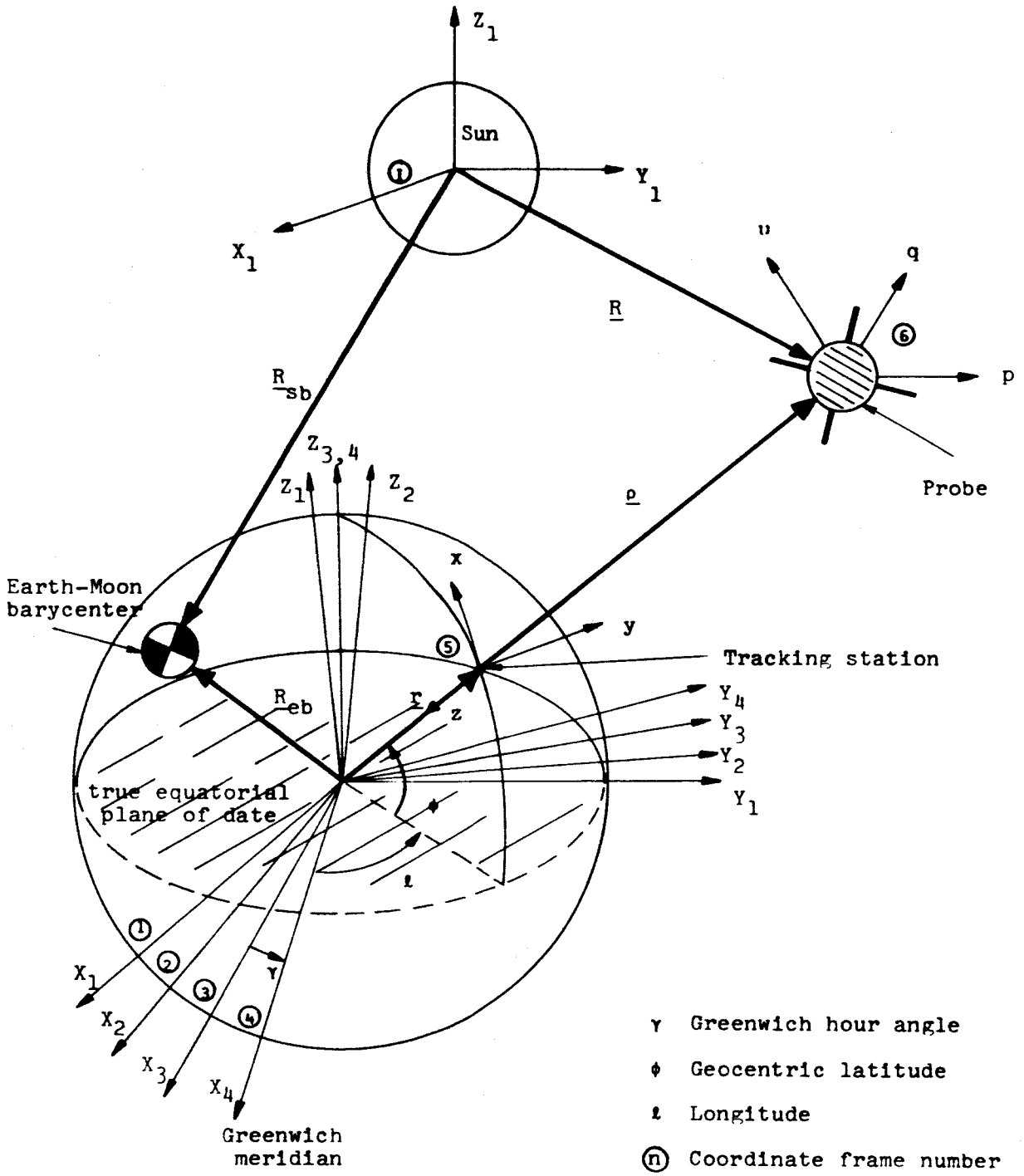
Z1
Sun
Y1
X1
R
R_sb
Z3,4
Z1
Z2
ρ
υ
q
p
Probe
Earth-Moon
barycenter
x
y
Tracking station
R_eb
r
z
Y4
Y3
Y2
Y1
true equatorial
plane of date
X1
X2
X3
X4
Greenwich
meridian
γ Greenwich hour angle
φ Geocentric latitude
ℓ Longitude
(n) Coordinate frame number

Figure 2.1

plane, the ecliptic, and the vernal equinox direction. The ecliptic is defined as the mean plane of the Earth's orbit around the Sun. The vernal equinox direction is defined by a line from the center of the Earth to the ascending node of the ecliptic in the equatorial plane or, in other words, to the point at which the Sun in its annual apparent path around the Earth crosses the equator from south to north. (8:24) The equator and ecliptic and hence the vernal equinox direction vary in spatial orientation due to the gravitational effect on the Earth of other celestial bodies.

The motion of the equatorial plane is due to the gravitational attraction of the Sun and Moon on the Earth's equatorial bulge and is commonly broken down into two separate motions. The first motion, nutation, is the rotation of the true polar axis about a mean polar axis with a period of approximately 18.6 years and a maximum amplitude of 9 seconds of arc. The second motion, luni-solar precession, is the rotation of the mean polar axis about the mean pole of the ecliptic with a period of approximately 26,000 years.

The motion of the ecliptic is due to the gravitational attraction of the planets on the Earth as a whole and is referred to as planetary precession. Due to this effect, the equinox precesses approximately 12 seconds of arc per century.

Luni-solar precession and planetary precession are normally considered jointly as a general precession. The combined result is a smooth, long term precession of the vernal equinox direction. For a more complete discussion of

nutation and precession, see References 8 and 17.

The orientations of the frames labeled 1, 2, 3, and 4 in Fig. 2.1 will be discussed in terms of the motions which have been described. The reference plane of frame 1 is the mean equatorial plane of the epoch 1950.0. This plane contains the X_1 axis, which is defined by the mean direction of vernal equinox at 1950.0. The Y_1 axis lies 90° east of X_1 in the reference plane, and Z_1 completes the Cartesian frame.

The reference plane of frame 2 is the mean equatorial plane at the time of interest, t, and the reference direction X_2 is the mean vernal equinox direction at t. The orientation between frames 1 and 2 depends upon the precessional motion of the equinox in the interval 1950.0 to t.

The reference plane of frame 3 is the true equatorial plane at time t, and the X_3 axis corresponds to the true direction of vernal equinox at t. The orientation between frames 2 and 3 is a function of the polar axis nutation. Since nutation and precession are very long term effects, frames 1, 2, and 3 will not differ from each other by more than a minute of arc in a 20 year interval.

Frame 4 differs from frame 3 by the Greenwich hour angle, γ, about the true polar axis $Z_{3,4}$. Frame 5 is a standard topocentric coordinate frame centered at the tracking station. The x and z axes lie in the local meridian plane with the z axis pointing toward the Earth's center and the x axis 90° from z in a northerly direction. The y axis points toward the east and completes the orthogonal triad. An

azimuth angle, A, is defined in frame 5 and will be measured from the x axis to the projection of $\underline{\rho}$ on the plane defined by the x and y axes. The elevation angle, L, is measured from the x-y plane to $\underline{\rho}$. At this point it is important to note that there are at least two frames to which measurements can be referred. In some instances, a measurement frame is defined such that the z axis lies along the Earth's gravity vector rather than pointing directly toward the Earth's center. The z axis of such a frame would deviate from the z axis of frame 5 by a small angle composed of two angles known as the deflection of the vertical and the deviation of the normal. For a more complete discussion of these angles, see References 6 and 10. The entire deviation will not usually be in the local meridian plane. It is possible to calculate the deviations analytically and align the measuring equipment such that frame 5 is instrumented. This is assumed to be the case in the development that follows. If, however, it is desired to instrument a frame defined by the gravity vector, an additional rotation matrix reflecting the difference between frame 5 and the actual measurement frame must be introduced.

Frame 6 is a probe centered, flight path coordinate system. The q axis of the frame is defined by the probe velocity vector while the u axis lies in the direction resulting from the cross produce $\underline{R} \times \underline{V}$. The p axis is then defined by $\underline{V} \times (\underline{R} \times \underline{V})$.

2.3 Expressing Position and Velocity Vectors in a Coordinate Frame

Because the ephemerides of the Moon and the Earth-Moon barycenter are available in inertial frame 1, the vector equation 2.5 will be coordinatized in this frame. It is convenient to express $\underline{\rho}$ in frame 5 and $\underline{r}$ in frame 4. Thus equation 2.5 with frame specification can be rewritten as

$$\underline{\rho}^{(1)} = C_2^1 C_3^2 C_4^3 C_5^4 \, \underline{\rho}^{(5)} \tag{2.6}$$

or

$$\underline{\rho}^{(1)} = \underline{R}^{(1)} + \underline{R}_{eb}^{(1)} - \underline{R}_{sb}^{(1)} - C_2^1 C_3^2 C_4^3 \, \underline{r}^{(4)} \tag{2.7}$$

The superscript indicates the frame in which the components of the position vectors are given, and C_j^k indicates a 3x3 transformation matrix from frame j to frame k. In frame 5 the components of $\underline{\rho}$ are

$$\underline{\rho}^{(5)} = \rho \begin{bmatrix} \cos L \cos A \\ \cos L \sin A \\ -\sin L \end{bmatrix} \tag{2.8}$$

In frame 4 the components of $\underline{r}$ are

$$\underline{r}^{(4)} = r \begin{bmatrix} \cos \phi \cos \ell \\ \cos \phi \sin \ell \\ \sin \phi \end{bmatrix} \tag{2.9}$$

The components of $\underline{R}_{sb}$ and $\underline{V}_{sb}$ in a Sun centered frame 1 and the components of the position and velocity vector of the Moon with respect to the Earth, $\underline{R}_{em}$ and $\underline{V}_{em}$, in an Earth centered frame 1 are obtained from the Jet Propulsion Laboratory Ephemeris Tapes described in Chapter 5 and in References 14

and 15. As mentioned earlier, $\underline{R}_{eb}$ and $\underline{V}_{eb}$ can be obtained readily from $\underline{R}_{em}$ and $\underline{V}_{em}$. Considering the definition of the mass center of two bodies,

$$m_m \underline{R}_{bm} = m_e \underline{R}_{eb} \tag{2.10}$$

$\underline{R}_{bm}$ is the position vector of the Moon with respect to the barycenter, and m_e and m_m are the masses of the Earth and Moon, respectively. Adding $\underline{R}_{eb} m_m$ to both sides of equation 2.10 yields

$$(m_e + m_m)\underline{R}_{eb} = m_m(\underline{R}_{eb} + \underline{R}_{bm}) \tag{2.11}$$

but $$\underline{R}_{eb} + \underline{R}_{bm} = \underline{R}_{em} \tag{2.12}$$

Therefore, in frame 1

$$\underline{R}_{eb}^{(1)} = \eta \underline{R}_{em}^{(1)} \tag{2.13}$$

and

$$\underline{V}_{eb}^{(1)} = \eta \underline{V}_{em}^{(1)} \tag{2.14}$$

where

$$\eta = m_m/(m_e + m_m) \tag{2.15}$$

The elements of the transformation matrices C_2^1 and C_3^2 are functions only of the time interval from 1950.0 to the current time of interest, t. Since these matrices deal with the extremely smooth, long term motions of precession and nutation, their time rates of change are taken to be zero.

The elements of the matrix C_4^3 are a function of the Greenwich hour angle, γ, which can also be expressed as a function of the time interval only. The time rate of change

of this matrix is again a function of γ and $\dot{\gamma}$ or ω, the Earth's rotation rate. The matrix C_5^4 is a function of latitude and longitude, and its time derivative is zero since the tracking station is fixed on the Earth's surface. Analytic expressions for all of the transformation matrices and their derivatives are given in Chapter 5.

In summary, the validity of the following expressions has been established.

$$\underline{\rho}^{(1)} = \underline{R}^{(1)} + {}_{\eta}\underline{R}^{(1)}_{em} - \underline{R}^{(1)}_{sb} - C_2^1 C_3^2 C_4^3 \, \underline{r}^{(4)} \qquad (2.16)$$

Differentiating with respect to time

$$\dot{\underline{\rho}}^{(1)} = \underline{V}^{(1)} + {}_{\eta}\underline{V}^{(1)}_{em} - \underline{V}^{(1)}_{sb} - C_2^1 C_3^2 \dot{C}_4^3 \, \underline{r}^{(4)} \qquad (2.17)$$

It has also been shown that given a specific time after the epoch 1950.0 and the geocentric position of the tracking station (ϕ and ℓ), the vector components of $\underline{R}^{(1)}_{em}$, $\underline{V}^{(1)}_{em}$, $\underline{R}^{(1)}_{sb}$, $\underline{V}^{(1)}_{sb}$, and $\underline{r}^{(4)}$ can be computed in the indicated frame along with the transformation matrices C_2^1, C_3^2, C_4^3, C_5^4, and $\dot{C}_4^3$. Thus if a nominal trajectory is specified for the probe in terms of $\underline{R}$ and $\underline{V}$, values for the components of $\underline{\rho}$ and $\dot{\underline{\rho}}$ could be computed from equations 2.16 and 2.17. It is also possible to obtain $\underline{\rho}^{(5)}$ and compute nominal values for the azimuth and elevation angles according to equation 2.8. These nominal values and the transformation matrices discussed will be used in the development of the maximum likelihood filter. It will also be necessary to use a transformation from frame 1 to frame 6. This transformation is discussed in Chapter 5.

CHAPTER 3

MEASUREMENTS AND THE NOMINAL TRAJECTORY

As will be shown later, certain measurements and statistical properties of the errors in these measurements can be used to make an estimate of the probe's state. This will be done in a manner that will minimize the mean square deviation of the state of the probe from some assumed nominal state. To do this, the state deviation must be related to the measurement deviations.

3.1 General Equations

In general, it can be written that a measurement is some function of the state.

$$m = f(\underline{x}) \tag{3.1}$$

Using the expression for $\underline{\rho}^{(5)}$ from equation 2.8 in equation 2.7, it is evident that the relationship expressed by equation 3.1 is nonlinear. For this reason a linearized Taylor Series is used. Expanding equation 3.1 in a Taylor Series about the nominal

$$m = m_N + \left[\frac{\partial f}{\partial \underline{x}}\right]_N (\underline{x} - \underline{x}_N)$$

$$+ \frac{1}{2}(\underline{x} - \underline{x}_N)^T \left[\frac{\partial}{\partial \underline{x}} \left(\frac{\partial f}{\partial \underline{x}}\right)^T\right]_N (\underline{x} - \underline{x}_N) + \ldots \tag{3.2}$$

Defining the deviations from the nominal,

$$\delta m = m - m_N \tag{3.3}$$

$$\delta \underline{x} = \underline{x} - \underline{x}_N \tag{3.4}$$

If the deviation from the nominal is small, then the series may be truncated and written

$$\delta m = \left[\frac{\partial f}{\partial \underline{x}}\right]_N \delta \underline{x} \tag{3.5}$$

The size of the deviation depends on how well the nominal trajectory fits the actual trajectory. This will be discussed when the determination of the nominal trajectory is considered.

In the case considered, the measurements are $\dot{\rho}$, A, and L, and the state to be determined is the $\underline{R}$ and $\underline{V}$ in equations 2.16 and 2.17. It is assumed that $\underline{R}_{em}$, $\underline{R}_{sb}$, $\underline{V}_{em}$, $\underline{V}_{sb}$, and $\underline{r}$ are well known so that their deviations from these known values are zero. $\underline{\rho}^{(5)}$ is a function of A, L, and $\dot{\rho}$ while the other vectors and transformation matrices are independent of the measured quantities.

Taking the variation of $\underline{R}$ with respect to $\dot{\rho}$, A, and L,

$$\delta \underline{R} = \frac{\partial \underline{R}}{\partial A} \delta A + \frac{\partial \underline{R}}{\partial L} \delta L + \frac{\partial \underline{R}}{\partial \dot{\rho}} \delta \dot{\rho} \tag{3.6}$$

3.2 Variation in Azimuth and Elevation

To get equation 3.6 in the desired form,

$$\delta m = f(\delta \underline{x}) = \underline{h}^T \delta \underline{x} \tag{3.7}$$

each variation must be examined separately. First, $\delta \underline{R}$ due to δA

$$\delta \underline{R} = \frac{\partial \underline{R}}{\partial A} \delta A \tag{3.8}$$

Taking the partial derivatives of the quantities in equation 2.1 with respect to A and noting that $\frac{\partial \underline{R}}{\partial A}_{ss} = 0$ yields

$$\frac{\partial \underline{R}}{\partial A} = \frac{\partial \underline{\rho}}{\partial A} \tag{3.9}$$

From equation 2.4

$$\frac{\partial \underline{\rho}}{\partial A}^{(5)} = \rho \begin{bmatrix} -\cos L \sin A \\ \cos L \cos A \\ 0 \end{bmatrix} \tag{3.10}$$

Dotting both sides of equation 3.8 with equation 3.10,

$$\frac{\partial \underline{\rho}}{\partial A} \delta \underline{R} = \frac{\partial \underline{\rho}}{\partial A}^{T} \frac{\partial \underline{\rho}}{\partial A} \delta A = \rho^2 \cos^2 L \, \delta A \tag{3.11}$$

Thus

$$\delta A = \frac{1}{\rho \cos L} \begin{bmatrix} -\sin A \\ \cos A \\ 0 \end{bmatrix} \delta \underline{R} \tag{3.12}$$

The coefficient of $\delta \underline{R}$ will be called the vector $\underline{a}$.

A similar analysis for δL yields

$$\delta L = \frac{1}{\rho} \begin{bmatrix} -\sin L \cos A \\ -\sin L \sin A \\ -\cos L \end{bmatrix} \delta \underline{R} \tag{3.13}$$

with

$$\frac{\partial \underline{\rho}}{\partial L}^{(5)} = \rho \begin{bmatrix} -\sin L \cos A \\ -\sin L \sin A \\ -\cos L \end{bmatrix} \tag{3.14}$$

and

$$\frac{\partial \underline{\rho}}{\partial L}^{T} \frac{\partial \underline{\rho}}{\partial L} = \rho^2 \tag{3.15}$$

3.3 Variation in Range Rate

To determine the relationship for range rate variation, $\delta\dot{\rho}$, an indirect approach must be used.

Taking the variation of equation 2.1 with $\delta\underline{R}_{ss} = 0$,

$$\delta\underline{R} = \delta\underline{\rho} \text{ (variation in position)} \tag{3.16}$$

Also

$$\delta\underline{V} = \delta\underline{\dot{\rho}} \text{ (variation in velocity)} \tag{3.17}$$

$\dot{\rho}$ is the rate of change of $\underline{\rho}$ in the $\underline{\rho}$ direction.

$$\dot{\rho} \neq |\underline{\dot{\rho}}| \tag{3.18}$$

$$\dot{\rho} = \frac{\underline{\rho}^T\underline{\dot{\rho}}}{\rho} \tag{3.19}$$

Also

$$\underline{\rho}^T\underline{\rho} = \rho^2 \tag{3.20}$$

Taking the time derivative of both sides of equation 3.20,

$$\underline{\dot{\rho}}^T\underline{\rho} + \underline{\rho}^T\underline{\dot{\rho}} = 2\rho\dot{\rho} \tag{3.21}$$

But

$$\underline{\dot{\rho}}^T\underline{\rho} = \underline{\rho}^T\underline{\dot{\rho}} \tag{3.22}$$

Thus

$$\underline{\rho}^T\underline{\dot{\rho}} = \rho\dot{\rho}$$

$$\dot{\rho} = \frac{\underline{\rho}^T\underline{\dot{\rho}}}{\rho} \tag{3.24}$$

Taking the variation,

$$\delta\dot{\rho} = \frac{\delta\underline{\rho}^T\underline{\dot{\rho}}}{\rho} + \frac{\underline{\rho}^T\delta\underline{\dot{\rho}}}{\rho} - \frac{\underline{\rho}^T\underline{\dot{\rho}}\delta\rho}{\rho^2} \tag{3.25}$$

Since each term is a scalar, it is equal to its transpose. Transposing the first term,

$$\delta\dot{\rho} = \frac{\underline{\dot{\rho}}^T\delta\underline{\rho}}{\rho} + \frac{\underline{\rho}^T\delta\underline{\dot{\rho}}}{\rho} - \frac{\underline{\rho}^T\underline{\dot{\rho}}\delta\rho}{\rho^2} \tag{3.26}$$

Taking the variation of equation 3.20,

$$\delta\underline{\rho}^T\underline{\rho} + \underline{\rho}^T\delta\underline{\rho} = 2\rho\delta\rho \tag{3.27}$$

$$2\underline{\rho}^T\delta\underline{\rho} = 2\rho\delta\rho \tag{3.28}$$

$$\delta\rho = \frac{\underline{\rho}^T\delta\underline{\rho}}{\rho} \tag{3.29}$$

Substituting equation 3.29 into 3.26,

$$\delta\dot{\rho} = \frac{\dot{\underline{\rho}}^T\delta\underline{\rho}}{\rho} + \frac{\underline{\rho}^T\delta\dot{\underline{\rho}}}{\rho} - \frac{(\underline{\rho}^T\dot{\underline{\rho}})\underline{\rho}^T\delta\underline{\rho}}{\rho^3} \tag{3.30}$$

$$\delta\dot{\rho} = \left[\frac{(\underline{\rho}^T\underline{\rho})\dot{\underline{\rho}}^T - (\underline{\rho}^T\dot{\underline{\rho}})\underline{\rho}^T}{\rho^3},\ \frac{\underline{\rho}^T}{\rho}\right]\begin{bmatrix}\delta\underline{\rho}\\ \delta\dot{\underline{\rho}}\end{bmatrix} \tag{3.31}$$

Substituting from equations 3.16 and 3.17 for $\delta\underline{\rho}$ and $\delta\dot{\underline{\rho}}$,

$$\delta\dot{\rho} = \underline{c}^T\begin{bmatrix}\delta\underline{R}\\ \delta\underline{V}\end{bmatrix} \tag{3.32}$$

3.4 H Matrix in the Measurement Frame

A measurement vector is defined

$$\underline{m} = \begin{bmatrix}A\\ L\\ \dot{\rho}\end{bmatrix} \tag{3.33}$$

$$\delta\underline{m} = \begin{bmatrix}\delta A\\ \delta L\\ \delta\dot{\rho}\end{bmatrix} = \tag{3.34}$$

$$\left[\begin{array}{cccccc}
\frac{-\sin A}{\rho\cos L}, & \frac{\cos A}{\rho\cos L}, & 0, & 0, & 0, & 0\\
\frac{-\cos A\sin L}{\rho}, & \frac{-\sin A\sin L}{\rho}, & \frac{-\cos L}{\rho}, & 0, & 0, & 0\\
\hline
\multicolumn{3}{c:}{\frac{(\underline{\rho}^T\underline{\rho})\dot{\underline{\rho}}^T - (\underline{\rho}^T\dot{\underline{\rho}})\underline{\rho}^T}{\rho^3}} & \multicolumn{3}{c}{\frac{\underline{\rho}^T}{\rho}}
\end{array}\right]\begin{bmatrix}\delta\underline{R}\\ \delta\underline{V}\end{bmatrix}$$

The matrix coefficient of $\delta\underline{x}$ is defined as H.

$$\delta\underline{m} = H\delta\underline{x} \tag{3.35}$$

The elements of H are evaluated along the nominal trajectory for the Taylor Series is expanded about the nominal state value.

3.5 Rotating into Flight Path Coordinates

For reasons stated in the following chapter, it is desirable to have the deviations in the flight path coordinate system. This requires that the elements of the H matrix be evaluated in the frame most convenient for computation and then rotated to the p-q-u frame.

This is easy to accomplish in the case of the third row of the H matrix. Since $\underline{\rho}$ and $\dot{\underline{\rho}}$ may be determined in the inertial frame (frame 1) from equations 2.16 and 2.17, they need only be transferred to the p-q-u frame.

$$\underline{\rho}^{(6)} = C_1^6\ \underline{\rho}^{(1)} \tag{3.36}$$

$$\dot{\underline{\rho}}^{(6)} = C_1^6\ \dot{\underline{\rho}}^{(1)} \tag{3.37}$$

Using these, the third row of the H matrix is written

$$\underline{h}_3^T = \left[\frac{(\underline{\rho}^T\underline{\rho})\dot{\underline{\rho}}^{(6)T} - (\underline{\rho}^T\dot{\underline{\rho}})\underline{\rho}^{(6)T}}{\rho^3},\ \frac{\underline{\rho}^{(6)T}}{\rho} \right] \tag{3.38}$$

The numerical calculation of $\underline{h}_3^T$ is accomplished in a slightly different manner in the flow chart of Chapter 5.

The first and second rows are conveniently evaluated in the measurement frame and will be called $\underline{a}^T$ and $\underline{b}^T$. (These

are the first three components; the last three in each row are zero. The zero elements are unchanged by the rotation.) These two vectors must be transferred to the flight path coordinate system.

$$\underline{h}_1^T = (C_1^6 C_2^1 C_3^2 C_4^3 C_5^4 \ \underline{a}^{(5)})^T \tag{3.39}$$

$$\underline{h}_2^T = (C_1^6 C_2^1 C_3^2 C_4^3 C_5^4 \ \underline{b}^{(5)})^T \tag{3.40}$$

The vector measurement deviation can then be written

$$\delta\underline{m} = \begin{bmatrix} \delta A \\ \delta L \\ \delta\dot{\rho} \end{bmatrix} = \begin{bmatrix} \underline{h}_1^T & \underline{0} \\ \underline{h}_2^T & \underline{0} \\ \underline{h}_3^T & \end{bmatrix} \begin{bmatrix} \delta\underline{R} \\ \delta\underline{V} \end{bmatrix} \tag{3.41}$$

The preceding derivations are similar to those presented by Madl (Ref. 13).

3.6 The Nominal Trajectory

Since the elements of H must be evaluated along a nominal trajectory, ρ, $\dot{\rho}$, $\underline{\rho}$, $\dot{\underline{\rho}}$, A, and L must be determined along the nominal. $\underline{\rho}$ and $\dot{\underline{\rho}}$ are obtained from equations 2.16 and 2.17 for $\underline{r}$, $\underline{R}_{em}$, $\underline{R}_{sb}$, $\underline{R}$, and their time derivatives are known time functions for a specified launch time and reference trajectory. ρ and $\dot{\rho}$ are scalars; hence, they are independent of frame. Writing $\underline{\rho}_N^{(5)}$,

$$\underline{\rho}_N^{(5)} = \rho_N \begin{bmatrix} \cos L_N \cos A_N \\ \cos L_N \sin A_N \\ -\sin L_N \end{bmatrix}$$

$$= \eta C_1^5 \underline{R}_{em}^{(1)} - C_1^5 \underline{R}_{sb}^{(1)} + C_1^5 \underline{R}_N^{(1)} - C_4^5 \underline{r}^{(4)} \tag{3.42}$$

The terms on the right are all calculable.

$$\underline{\rho}_N^{(5)} = \begin{bmatrix} x \\ y \\ z \end{bmatrix} \tag{3.43}$$

where x, y, and z are the numbers calculated.

$$\rho_N = \sqrt{x^2 + y^2 + z^2} \tag{3.44}$$

$$L_N = \sin^{-1}\left[\frac{-z}{\sqrt{x^2 + y^2 + z^2}}\right] \tag{3.45}$$

$$A_N = \sin^{-1}\left[\frac{y}{\cos L_N \sqrt{x^2 + y^2 + z^2}}\right] \tag{3.46}$$

$$\dot{\rho}_N = \frac{\underline{\rho}_N^T \dot{\underline{\rho}}_N}{\rho_N} \tag{3.47}$$

These are all of the quantities needed to evaluate the H matrix at all points along the trajectory.

Thus far, it has been assumed that a nominal trajectory for the state has been given. This reference trajectory is quite important for if the deviation from it is very large, the truncation of the Taylor Series is not valid. The term $\delta\underline{x}^2$ and those of higher order become significant. To obtain the most accurate H matrix possible, it would be necessary to compute the reference trajectory by numerically solving the many body equations of motion in some manner similar to the one described in JPL Tech. Report 32-223(Ref. 10). Several simpler alternatives exist. The simplest assumption is

that the probe is in an elliptical orbit about the Sun which is determined by the burnout conditions. Another method would be to use an on-board transponder to infer vehicle position and velocity after burnout until the Earth's sphere of influence is reached. A solar orbit could be defined at that point.

CHAPTER 4

MAXIMUM-LIKELIHOOD ESTIMATION

Several authors have described the theory of maximum-likelihood estimation (Bryson, Battin, Kalman, etc.). Only an outline of this theory will be given here, and the assumptions peculiar to the study of this thesis will be discussed. The method presented here is essentially that given by Bryson (Ref. 3).

4.1 Deviation Equation

It is desired to estimate the elements of the state deviation vector, $\delta\underline{x}$, using knowledge of the deviations of certain measurable quantities, $\delta\underline{m}$, from nominal values. The measurable quantities contain random errors which have known statistical properties. In equation form

$$\delta\underline{m} = H\delta\underline{x} + \underline{v} \tag{4.1}$$

The H matrix is that developed in the third chapter, and $\underline{v}$ is the measurement noise vector.

4.2 Error Covariance Matrices

To proceed, statistical knowledge of the measurement noise is required. Thus

$$E(\underline{v}\underline{v}^T) = R \tag{4.2}$$

The expected value of the noise vector times its transpose

is a positive definite matrix, R. That is, over many measurements the diagonal elements of the R matrix will reflect the square of the standard deviations of the individual measurements. Also, some estimate of the deviation is needed such that

$$E\left[(\delta\underline{x} - \delta\underline{\bar{x}})(\delta\underline{x} - \delta\underline{\bar{x}})^T\right] = M \qquad (4.3)$$

$\delta\underline{x}$ is the true state deviation which is inaccessible and never known. $\delta\underline{\bar{x}}$ is the estimated state deviation before a measurement, and M is an n x n positive definite matrix where n is the dimension of the state.

4.3 Weighted Least-Squares Estimate

A weighted least-squares estimate, $\delta\underline{x}$, of the state deviation is found by minimizing the quadratic form

$$J = \frac{1}{2}(\delta\underline{x} - \delta\underline{\bar{x}})^T M^{-1}(\delta\underline{x} - \delta\underline{\bar{x}}) + (\delta\underline{m} - H\delta\underline{x})^T R^{-1}(\delta\underline{m} - H\delta\underline{x}) \qquad (4.4)$$

The weighting matrices M^{-1} and R^{-1} are the inverses of the matrices that reflect the statistical properties described before.

Bryson proceeds to show that the $\delta\underline{x}$ chosen to minimize this quadratic form is also that which is the maximum-likelihood or minimum-variance estimate.

For convenience, this abbreviated notation will be used in the development that follows.

$$\delta \underline{x} \sim \underline{x}$$

$$\delta \bar{\underline{x}} \sim \bar{\underline{x}}$$

$$\delta \hat{\underline{x}} \sim \hat{\underline{x}}$$

$$\delta \underline{m} \sim \underline{m}$$

It is desired to minimize

$$J = \frac{1}{2}\left[(\underline{x} - \bar{\underline{x}})^T M^{-1}(\underline{x} - \bar{\underline{x}}) + (\underline{m} - H\underline{x})^T R^{-1}(\underline{m} - H\underline{x})\right] \quad (4.5)$$

Taking the differential,

$$dJ = d\underline{x}^T \left[M^{-1}(\underline{x} - \bar{\underline{x}}) - H^T R^{-1}(\underline{m} - H\underline{x})\right] \quad (4.6)$$

If dJ is to vanish for an arbitrary $d\underline{x}$, the coefficient of $d\underline{x}^T$ must be equal to zero.

$$\left[M^{-1}(\underline{x} - \bar{\underline{x}}) - H^T R^{-1}(\underline{m} - H\underline{x})\right] = 0 \quad (4.7)$$

Rearranging and calling the $\underline{x}$ that satisfies equation 4.7 the best estimate $\hat{\underline{x}}$

$$(M^{-1} + H^T R^{-1} H)\hat{\underline{x}} = H^T R^{-1}\underline{m} + M^{-1}\bar{\underline{x}} \quad (4.8)$$

Adding and subtracting $H^T R^{-1} H\bar{\underline{x}}$ from the right-hand side,

$$(M^{-1} + H^T R^{-1} H)\hat{\underline{x}} = H^T R^{-1}(\underline{m} - H\bar{\underline{x}}) + (M^{-1} + H^T R^{-1} H)\bar{\underline{x}} \quad (4.9)$$

Defining a matrix P such that

$$P^{-1} = M^{-1} + H^T R^{-1} H \quad (4.10)$$

and multiplying both sides of equation 4.9 by P,

$$\hat{\underline{x}} = \bar{\underline{x}} + PH^T R^{-1}(\underline{m} - H\bar{\underline{x}}) \quad (4.11)$$

Or in deviation notation, 4.11 is written

$$\delta\underline{\hat{x}} = \delta\underline{\bar{x}} + PH^{T}R^{-1}(\delta\underline{m} - H\delta\underline{\bar{x}}) \qquad (4.12)$$

The best estimate of the deviation after a measurement has been taken depends on an estimate of the deviation before the measurement, $\delta\underline{\bar{x}}$, the measurement deviation, $\delta\underline{m}$, and the P, H, and R matrices. The H matrix has been described before as relating the state deviations to the measurement deviations and is evaluated along the nominal trajectory. The R matrix is known from characteristics of the measuring system. The P matrix, which has only been defined thus far, is the error covariance matrix of the estimated deviation.

4.4 Error Covariance Matrix After Measurement

The error, $\underline{e}$, is defined as

$$\underline{e} = \delta\underline{\hat{x}} - \delta\underline{x} \qquad (4.13)$$

It will be shown that

$$P = E\left[(\delta\underline{\hat{x}} - \delta\underline{x})(\delta\underline{\hat{x}} - \delta\underline{x})^{T}\right] \qquad (4.14)$$

Using the abbreviated notation,

$$\underline{e} = \underline{\hat{x}} - \underline{\bar{x}} + \underline{\bar{x}} - \underline{x} \qquad (4.15)$$

Rearranging

$$\underline{e} = \underline{\bar{x}} - \underline{x} + (\underline{\hat{x}} - \underline{\bar{x}}) \qquad (4.16)$$

From equation 4.11

$$\underline{\hat{x}} - \underline{\bar{x}} = PH^{T}R^{-1}(\underline{m} - H\underline{\bar{x}}) \qquad (4.17)$$

$$\underline{e} = \underline{\bar{x}} - \underline{x} + PH^{T}R^{-1}(\underline{m} - H\underline{\bar{x}}) \qquad (4.18)$$

Using

$$\underline{m} = H\underline{x} + \underline{v} \tag{4.19}$$

$$\underline{e} = \bar{\underline{x}} - \underline{x} + PH^TR^{-1}\left[H(\underline{x} - \bar{\underline{x}}) + \underline{v}\right] \tag{4.20}$$

Rearranging

$$\underline{e} = (I - PH^TR^{-1}H)(\bar{\underline{x}} - \underline{x}) + PH^TR^{-1}\underline{v} \tag{4.21}$$

For convenience, define a matrix K such that

$$K \equiv PH^TR^{-1} \tag{4.22}$$

$$\underline{e} = (I - KH)(\bar{\underline{x}} - \underline{x}) + K\underline{v} \tag{4.23}$$

If the deviations and the noise are assumed to be independent, that is,

$$E(\underline{v}\underline{x}^T) = E(\underline{x}\underline{v}^T) = E(\bar{\underline{x}}\underline{v}^T) = E(\underline{v}\bar{\underline{x}}^T) = 0 \tag{4.24}$$

then

$$E(\underline{e}\underline{e}^T) = E\left[[(I - KH)(\bar{\underline{x}} - \underline{x}) + K\underline{v}][(I - KH)(\bar{\underline{x}} - \underline{x}) + K\underline{v}]^T\right] \tag{4.25}$$

Expanding

$$\begin{aligned} E(\underline{e}\underline{e}^T) = E\Big[&(I - KH)(\bar{\underline{x}} - \underline{x})(\bar{\underline{x}} - \underline{x})^T(I - KH)^T \\ &+ (I - KH)(\bar{\underline{x}} - \underline{x})(K\underline{v})^T \\ &+ K\underline{v}(\bar{\underline{x}} - \underline{x})^T(I - KH)^T + K\underline{v}\underline{v}^TK^T\Big] \end{aligned} \tag{4.26}$$

Using equations 4.2, 4.3, and 4.27,

$$E(\underline{e}\underline{e}^T) = (I - KH)M(I - KH)^T + KRK^T \tag{4.27}$$

Premultiplying equation 4.10 by P and postmultiplying by M,

$$M = P + PH^T R^{-1} HM = P + KHM \tag{4.28}$$

Or

$$(I - KH)M = P \tag{4.29}$$

Substituting into equation 4.29,

$$E(\underline{e}\underline{e}^T) = P - PH^T K^T + KRK^T \tag{4.30}$$

Using the definition of K from equation 4.24,

$$E(\underline{e}\underline{e}^T) = P + (PH^T R^{-1} R - PH^T)K^T \tag{4.31}$$

$$E(\underline{e}\underline{e}^T) = P + (PH^T - PH^T)K^T \tag{4.32}$$

$$E(\underline{e}\underline{e}^T) = P \tag{4.33}$$

This is the desired result. The P matrix is the error covariance matrix of the difference between the estimated and the actual state deviations (equation 4.16). Another way of stating this is that P is the error covariance matrix after incorporation of a measurement.

4.5 Updating with the State Transition Matrix

The case being considered is best described by

$$\delta\underline{x}_{i+1} = \overline{\Phi}_i \delta\underline{x}_i + \Gamma_i \delta\underline{u}_i \tag{4.34}$$

$\delta\underline{x}_i$ is the state deviation at one time, and $\delta\underline{x}_{i+1}$ is the deviation at a later time. $\delta\underline{u}_i$ is a vector forcing function. For the present, the forcing vector will be considered identically zero. Thus

$$\delta\underline{x}_{i+1} = \underline{\Phi}_i \delta\underline{x}_i \tag{4.35}$$

$\underline{\Phi}_i$ is the state transition matrix from time t_i to t_{i+1}, and would be more completely written $\underline{\Phi}(t_{i+1},t_i)$. It is either a known analytical function of time or may be found numerically.

It follows that the best estimate at a given stage before measurement $\delta\bar{\underline{x}}_i$ is the best estimate after the last measurement updated with the state transition matrix.

$$\delta\bar{\underline{x}}_i = \underline{\Phi}_{i,i-1}\delta\hat{\underline{x}}_{i-1} \tag{4.36}$$

It follows also that the best error covariance matrix before measurement at state i is the error covariance matrix after the last measurement updated by the transition matrix.

$$M_i = \underline{\Phi}_{i,i-1} P_{i-1} \underline{\Phi}^T_{i,i-1} \tag{4.37}$$

(Both equations 4.38 and 4.39 are written assuming that the disturbing force is equal to zero.)

Henceforth, $\underline{\Phi}_i$ will denote the transition from state t_i to t_{i+1} and $\underline{\Phi}_i^{-1}$ will denote the transition from t_{i+1} to t_i.

4.6 Initial Conditions

If it is assumed that the best estimate of the state deviation before the first measurement is equal to zero,

$$\delta\bar{\underline{x}}_o = 0 \tag{4.38}$$

then the initial error covariance matrix before measurement is given by

$$E(\delta\underline{x}_o \delta\underline{x}_o^T) = M_o \tag{4.39}$$

For the mission proposed for the first Sunblazer probe, Ling-Temco-Vought has estimated the standard deviations of the injection conditions. Madl used these deviations to compute initial state deviations. So that a comparison can be made and because the LTV report is the best available information, the same numbers used by Madl for the initial error covariance matrix will be used here. They are as follows:

$$\sigma_{Rp}^2 = \sigma_{Rq}^2 = \sigma_{Ru}^2 = 10.7 \times 10^{-8} \text{ AU}^2$$

$$\sigma_{Vp} = \sigma_{Vu}^2 = 15.3 \times 10^{-4} \text{ (AU/Yr)}^2$$

$$\sigma_{Vq}^2 = 2.9 \times 10^{-4} \text{ (AU/Yr)}^2 \qquad (4.40)$$

These are the diagonal terms of the error covariance matrix at injection written in frame 6 or the flight path coordinate system. The assumptions made by Madl still apply. That is, the error in position at burnout and the error in velocity at burnout in the p-u plane are independent of direction.

The R matrix is a function of the devices used for taking the measurements. The error in each separate measurement is assumed to be independent of the others so that the R matrix is a diagonal matrix (all the elements off the main diagonal are equal to zero). Madl assumed a one-tenth degree variation in the two angle measurements and varied the quality of the range rate data to determine its effect. The same procedure will be used here. These variances will be assumed constant over the entire flight. If knowledge of the

change in the variances with time were available, it could be included in the filter and would improve the estimate of the state deviation.

4.7 Recursive Estimation

Knowing the initial deviation error covariance matrix, M_o (o denotes injection), a measurement must be taken at injection to determine the P_o matrix.

$$P_o^{-1} = M_o^{-1} + H_o^T R^{-1} H_o \tag{4.41}$$

$$\delta\hat{\underline{x}}_o = \delta\bar{\underline{x}}_o + P_o H_o^T R^{-1}(\delta\underline{m}_o - H_o \delta\bar{\underline{x}}_o) \tag{4.42}$$

Or

$$\delta\hat{\underline{x}}_o = P_o H_o^T R^{-1} \delta\underline{m}_o \tag{4.43}$$

since $\delta\bar{\underline{x}}_o$ has been assumed equal to zero.

For the next measurement,

$$M_1 = \bar{\Phi}_o P_o \bar{\Phi}_o^T \tag{4.44}$$

$$\delta\bar{\underline{x}}_1 = \bar{\Phi}_o \delta\hat{\underline{x}}_o \tag{4.45}$$

$$P_1^{-1} = M_1^{-1} + H_1^T R^{-1} H_1 \tag{4.46}$$

This process is repeated for as many measurements as desired. It is evident that measuring on the average decreases the uncertainty in the estimate of the state deviation. Looking at equation 4.10, M^{-1} is a positive definite matrix, and the $H^T R^{-1} H$ matrix is also positive definite. Thus each measurement increases the previously updated P^{-1} matrix and

decreases the P matrix. This P matrix establishes the quality of the estimation of the state deviation.

For simulation purposes actual measurement data are not available. However, since the M_o and the R matrices are available, and the H matrix is evaluated along the nominal trajectory, it is possible to calculate the error covariance matrix, P, at conjunction. This is what Madl calls his "Figure of Merit" (13:31). As stated before, this error covariance matrix indicates the accuracy of the estimate of the state deviation found when using actual data. A P matrix at conjunction was computed, and the results are compared with Madl's in Chapter 6.

4.8 State Transition Matrix

Thus far, nothing has been said about the state transition matrix, $\underline{\Phi}_i$. This matrix is determined by the choice of a nominal orbit for the probe. Since a two body orbit has a state transition matrix whose elements are analytic functions of time, this is the nominal orbit chosen for the computation of the results in Chapter 6. A more accurate result might be obtained by assuming the nominal orbit to be a many body problem with the Sun as the principal body. This would complicate the calculations a great deal. Either the state transition matrix would have to be determined numerically, or the disturbing function, $\underline{u}_i$, in equation 4.36 would be a nonzero vector, and a Γ_i matrix would have to be found. Numerical integration would be necessary in either case.

Since a program written by Mr. Jack Fagan for calculating the error covariance matrix was available, the two body assumption for a nominal probe orbit was used. This seems justified for the purposes of this study and would be justified in the actual processing of data if the state deviation remained small. Mr. Fagan's program uses an analytical state transition matrix in the flight path coordinate system. This is why the p-q-u coordinate system was defined. The flow chart presented in Chapter 5 presumes a state transition matrix based on many body theory.

4.9 Prediction

Measurements cannot be taken continually through conjunction for the effects of the corona of the Sun destroy the transmission of the radio signal. Madl determined that the two-week period on either side of conjunction was the only time when measurements could not be taken. His criteria will be used here. From this it is apparent that some method must be used to determine the state deviation during this period for this is when it must be known. The last measurements will be taken two weeks before conjunction. The best estimate of the state deviation from that time until two weeks after conjunction will be the best estimate after the last measurement updated with the state transition matrix.

$$\delta\hat{\underline{x}}_{t_d} = \underline{\Phi}(t_d,\tau)\,\delta\hat{\underline{x}}_{\tau} \qquad (4.48)$$

t_d is the time during the conjunction phase of the flight

when knowledge of the deviation is desired, and τ is the time of conjunction minus two weeks.

The P matrix does not depend on the actual measurements and may be calculated for any point along the trajectory. However, since no measurements may be taken for a four-week period, the best indication of the certainty of the estimated state deviation during this period is the error covariance matrix after the last measurement, P_τ, updated with the state transition matrix.

$$P_{t_d} = \Phi(t_d,\tau)P\,\Phi^T(t_d,\tau) \qquad (4.49)$$

(Both equations 4.48 and 4.49 are valid only for the period when no measurements are available.)

4.10 Summary

To review, a method has been developed to recursively estimate the state deviation along some nominal orbit using measurement data. This procedure requires knowledge of the initial deviation error covariance matrix and the error covariance matrix of measurement deviations. It has been assumed that (1) the measurement errors are uncorrelated which makes the measurement error correlation matrix diagonal, (2) the measurement noise and the state deviation are uncorrelated which makes the P matrix the error covariance matrix after measurement, and (3) the assumptions stated before concerning the initial injection errors still apply. This allows the computation of the initial M matrix.

All quantities except the actual measurements and the updated best estimate of the state deviation may be precalculated. That is, with an assumed nominal orbit, the H_i and P_i matrices may be calculated. Also the nominal measurement values, $\underline{m}_N$, may be calculated. To process the actual data, the measurements must be taken and used with the precalculated nominal measurements to get the measurement deviations.

$$\underline{m} - \underline{m}_N = \delta\underline{m} \tag{4.50}$$

Then the previous best estimate is updated, and the current best estimate is obtained (equations 4.45 and 4.47).

CHAPTER 5

STATE ESTIMATION PROGRAM

The state estimation program which is described in this chapter will be considered in two parts. (Henceforth, for convenience, this program will be referred to as SPADAF for SPAce DAta Filtering.)

5.1 General Description

In the first part of the program, the nominal measurement values and the elements of the H matrix in frame 6 are calculated. The motions of the Earth described in Chapter 2 are taken into account along with the motion of the probe on its nominal trajectory. The transformation matrices defined in Chapter 2 are computed in the subroutines labeled TR1, TR2, TR3, and TR6. These subroutines, along with the subroutine TRAFER, which multiplies a three-component column vector by a 3x3 matrix, and the JPL Ephemeris Tapes, are discussed in sections 5.6 and 5.7.

The second portion of SPADAF makes use of the results obtained in part one to filter actual measurement data in real time and thus arrive at an estimate of the probe's state in frame 6. The equations for the estimation are presented in Chapter 4 and are repeated in the SPADAF flow chart, which is presented in section 5.5.

In both parts of SPADAF, information based on a predesignated nominal trajectory is needed. $\underline{R}_N$ and $\underline{V}_N$ are required in the calculation of H, while in the filtering section, it is necessary to know the state transition matrix along the nominal trajectory. Several methods exist for calculating $\underline{R}_N$, $\underline{V}_N$, and $\underline{\underline{\Phi}}$. The simplest of these would be based on a two body assumption, while the most complicated would take into account the influence of each planet in the solar system. Programs are available at the Center for Space Research which compute the required nominal quantities at any time past injection. These programs take into consideration the major perturbing effects that would be encountered by the probe.

Preceding the flow chart is a list of the inputs necessary to process measurements for a particular case. The inputs are described in the listing with sufficient detail except for the time inputs. Since practically all of the quantities computed in SPADAF will be time dependent, it is important to choose a consistent and an accurate system of time. This will be discussed in section 5.3.

5.2 Possible Changes

There appear to be two possible changes to SPADAF that may be desirable or necessary in the future. The first change arises when the frame in which the measurements are taken deviates slightly from frame 5. This was discussed in Chapter 2.

The second change arises when it appears that the computed estimate of the state deviation, $\delta\hat{\underline{x}}$, becomes large enough to invalidate equation 3.5. To correct this situation, it may be necessary to check the magnitude of $\delta\hat{\underline{x}}$ at each measurement and redefine the nominal trajectory based on the best estimate of the true state, $\hat{\underline{x}}$, at the time $\delta\hat{\underline{x}}$ approaches the point where equation 3.5 is no longer valid.

5.3 Systems of Time Determination

The purpose of this section is merely to introduce some of the concepts used in the determination of time and to provide a basis for understanding the time inputs required in SPADAF. For a complete and authoritative survey of time systems, see Reference 8.

Prior to the discovery that the Earth's rotation rate, ω, is variable, periods of time were defined by the relative positions of celestial bodies with respect to the Greenwich meridian. These time systems are not uniform since the length of a solar or a sidereal day varies. The desire for a uniform measure of time led to the adoption of Ephemeris time (ET) in 1958.

Currently, there are three commonly used time systems, which are as follows:

1. Universal time (UT) is defined by the diurnal (daily), nonuniform motion of the Earth with respect to the Sun.
2. Sidereal time is defined by the diurnal, nonuniform motion of the Earth with respect to the stars.

3. Ephemeris time (ET) is defined by the laws of dynamics. The lengths of the various time units in this system are fixed by definition.

Sidereal time and universal time are related by a numerical formula, while UT and ET differ by the varying quantity ΔT which must be determined empirically. In practice, ΔT is determined from observed motions of the Moon.

To provide a continuous count of the days that have passed since an epoch far in the past, the concept of the Julian date was established by astronomers. A Julian day number has been assigned to each day, beginning at Greenwich noon (12^h), that has elapsed since January 1, 4713 B.C. The Julian date of any instant in time past the 4713 B.C. epoch includes the Julian day number plus the fraction of the day past 12^h.

Originally, the Julian day count was intended to be a continuous count of mean solar days. Although ephemeris time is uniform, it is still possible to use a similar continuous day count based on ET. Since the beginning of ephemeris time was defined as January 0^d 12^h 1900 (ET), the Julian date (UT) is very close to the Julian date (ET) at that instant. Because of this definition, ΔT is small at the 1900 epoch but begins to grow as time progresses from that epoch.

The Ephemeris Tapes used in SPADAF are based on an epoch defined by the beginning of the Besselian year 1950. This

epoch is denoted by 1950.0 and is determined by the position relative to the Earth of an imaginary point (fictitious sun) on the mean celestial equator. The Julian date (ET) corresponding to 1950.0 is 243 3282.423357.

5.4 Program Inputs

1. Geocentric latitude, ϕ, and longitude, ℓ, of the tracking station in degrees.
2. Initial (injection) position, $\underline{R}_o$(AU), and velocity, $\underline{V}_o$(AU/Yr), of the probe relative to the Sun in frame 1.
3. Error covariance matrix at injection M_o(AU and AU^2/Yr^2).
4. Measurement error correlation matrix R(AU^2/Yr^2 and rad^2).
5. Magnitude of the Earth's radius $\underline{r}$ at the tracking station in AU.
6. Julian date (UT) of injection in days.
7. Julian date (UT) of the measurement in days.
8. Correction factor ΔT to convert universal time to ephemeris time in days.
9. The measurements A, L, and $\dot{\rho}$ in rad and AU/Yr.
10. JPL Ephemeris Tapes.
11. Subroutines or tapes to provide the nominal $\underline{R}$, $\underline{V}$, and $\underline{\Phi}$ at the measurement times.

5.5 SPADAF Flow Chart

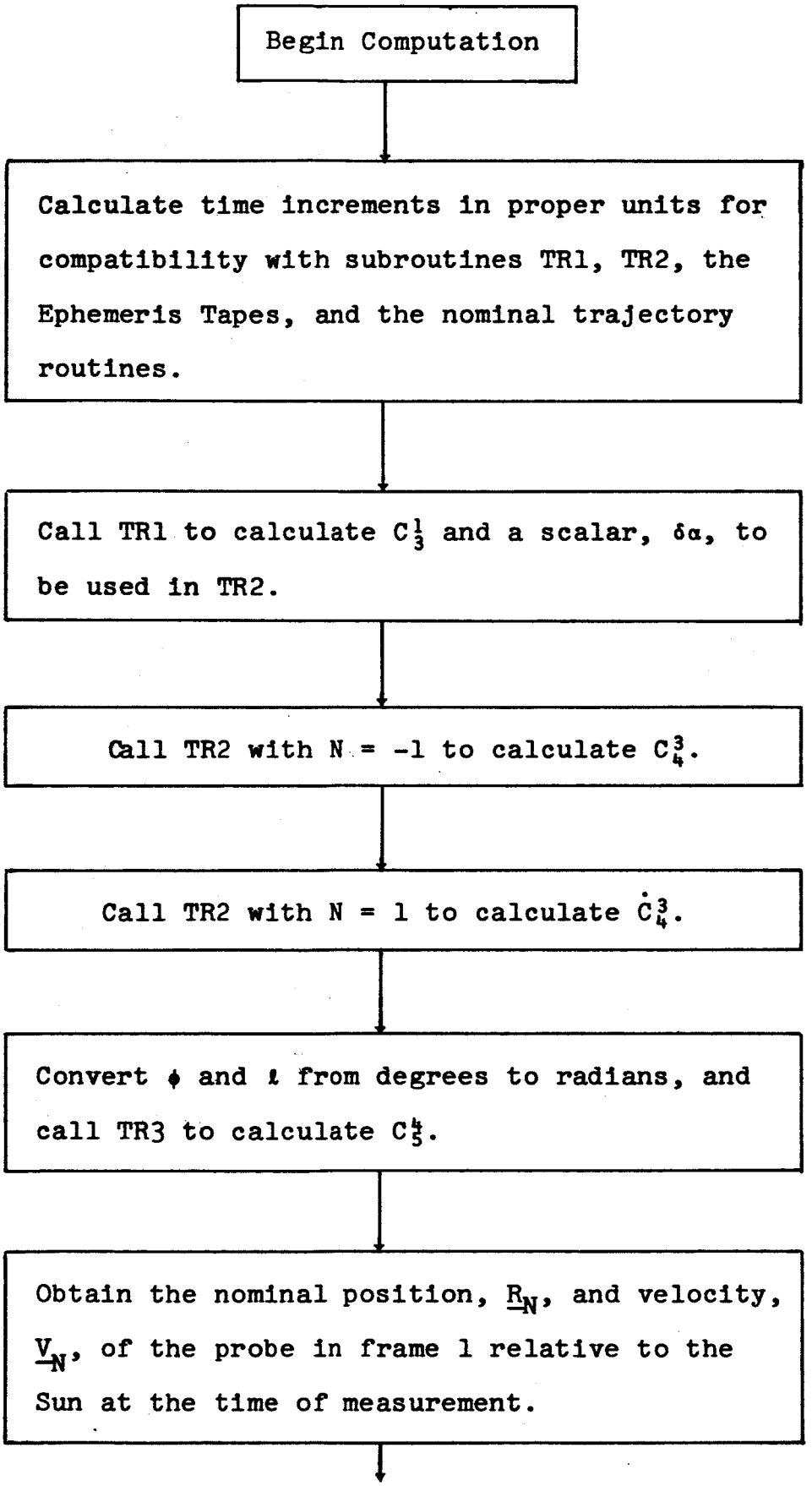

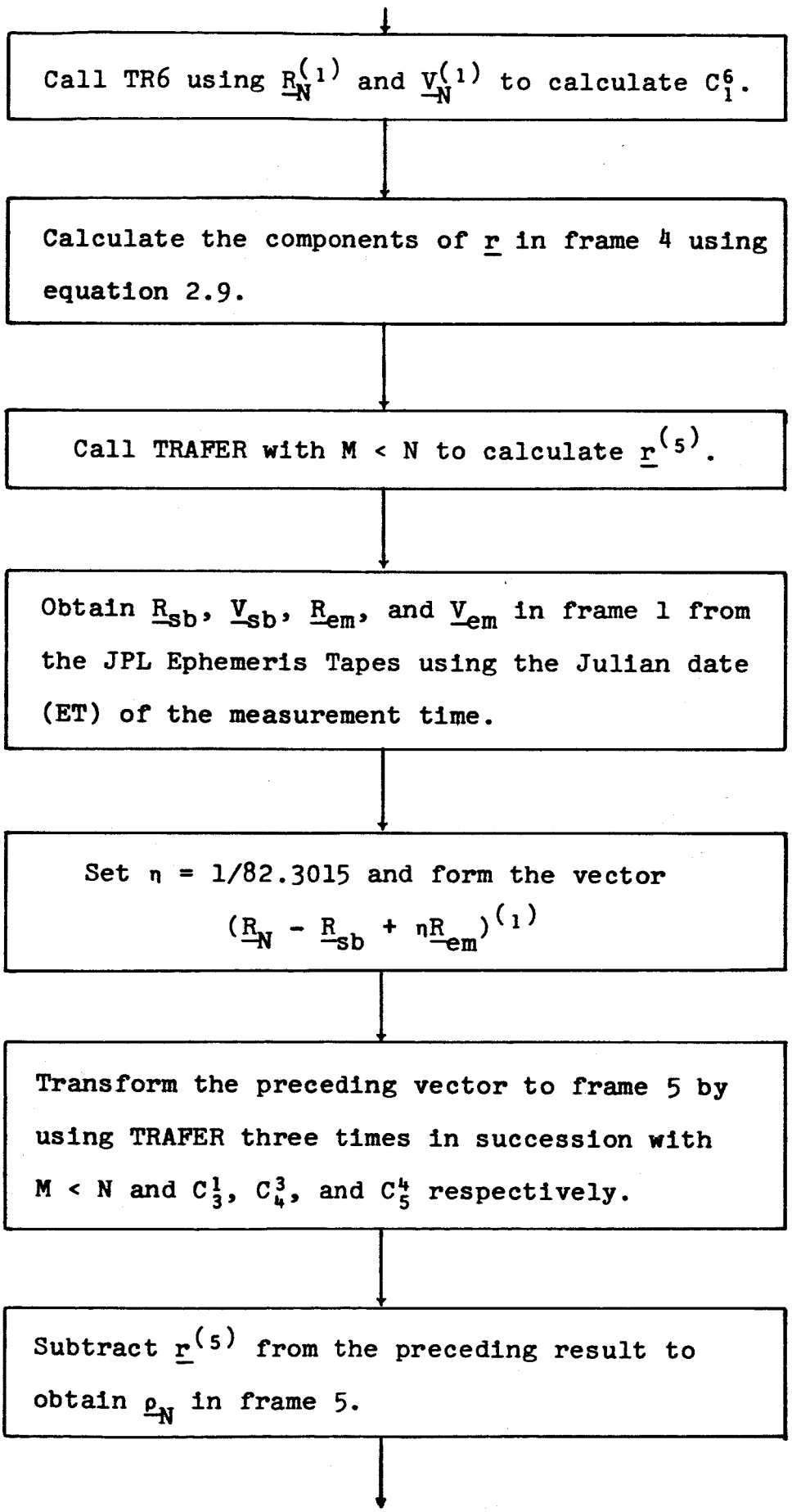
Call TR6 using $\underline{R}_N^{(1)}$ and $\underline{V}_N^{(1)}$ to calculate C_1^6.
Calculate the components of $\underline{r}$ in frame 4 using equation 2.9.
Call TRAFER with M < N to calculate $\underline{r}^{(5)}$.
Obtain $\underline{R}_{sb}$, $\underline{V}_{sb}$, $\underline{R}_{em}$, and $\underline{V}_{em}$ in frame 1 from the JPL Ephemeris Tapes using the Julian date (ET) of the measurement time.
Set $\eta = 1/82.3015$ and form the vector $(\underline{R}_N - \underline{R}_{sb} + \eta\underline{R}_{em})^{(1)}$
Transform the preceding vector to frame 5 by using TRAFER three times in succession with M < N and C_3^1, C_4^3, and C_5^4 respectively.
Subtract $\underline{r}^{(5)}$ from the preceding result to obtain $\underline{\rho}_N$ in frame 5.

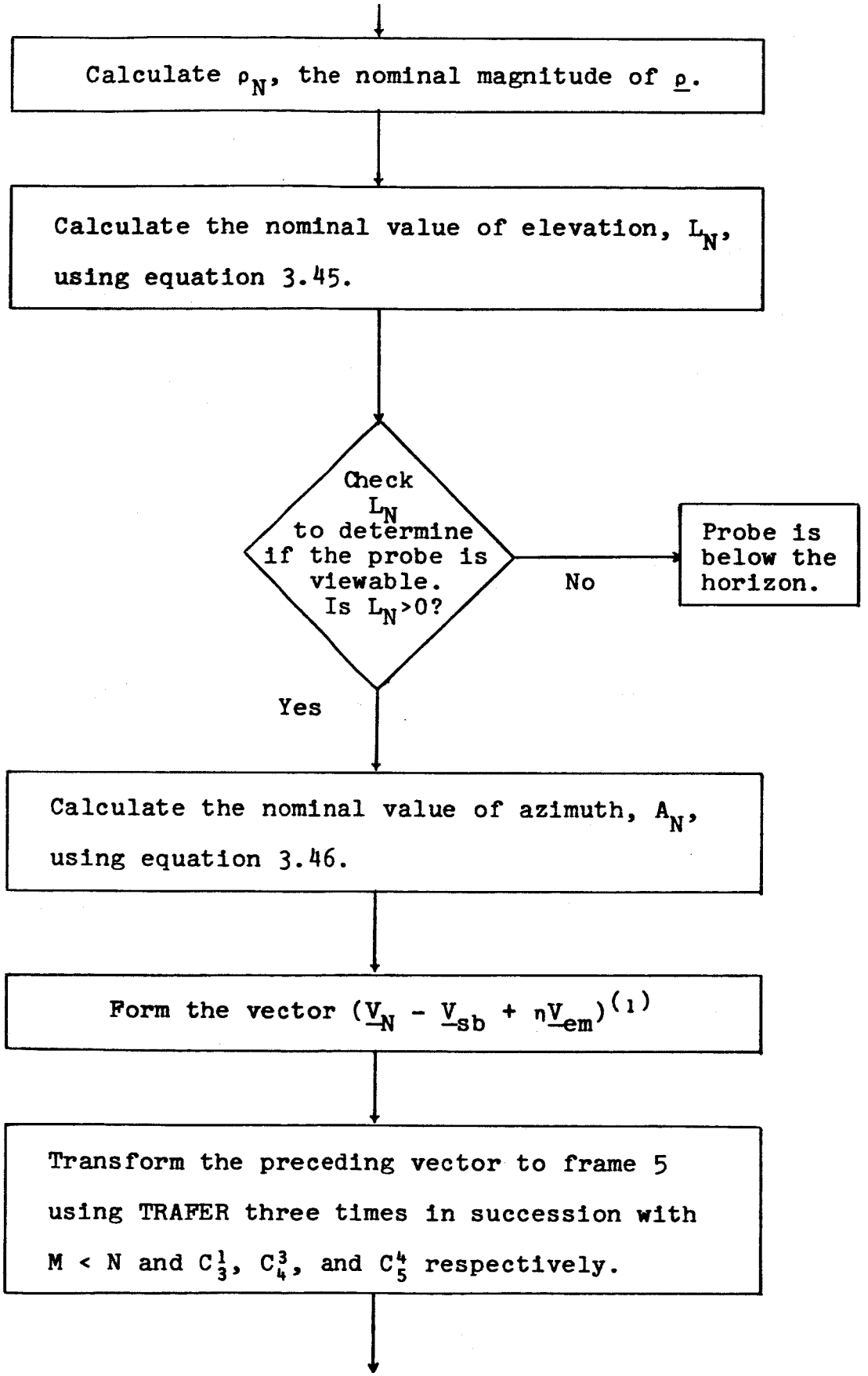
Calculate ρ_N, the nominal magnitude of $\underline{\rho}$.
Calculate the nominal value of elevation, L_N, using equation 3.45.
Check L_N to determine if the probe is viewable. Is $L_N > 0$?
No
Probe is below the horizon.
Yes
Calculate the nominal value of azimuth, A_N, using equation 3.46.
Form the vector $(\underline{V}_N - \underline{V}_{sb} + n\underline{V}_{em})^{(1)}$
Transform the preceding vector to frame 5 using TRAFER three times in succession with M < N and C_3^1, C_4^3, and C_5^4 respectively.

Transform the vector $(\underline{R}_N - \underline{R}_{sb} + \eta\underline{R}_{em})^{(1)}$ to frame 5 using TRAFER three times in succession with $M < N$ and C_3^1, $\dot{C}_4^3$, and C_5^4 respectively.

Calculate the nominal value of $\dot{\underline{\rho}}^{(5)}$.

$$\dot{\underline{\rho}}_N^{(5)} = C_4^5 C_3^4 C_1^3 (\underline{V}_N - \underline{V}_{sb} + \eta\underline{V}_{em})^{(1)} + C_4^5 \dot{C}_3^4 C_1^3 (\underline{R}_N - \underline{R}_{sb} + \eta\underline{R}_{em})^{(1)}$$

Calculate the nominal value of $\dot{\rho}$.

$$\dot{\rho}_N = (\underline{\rho}_N^T \dot{\underline{\rho}}_N)/\rho_N$$

Calculate the first two rows of the H matrix in frame 5.

$$H_{11} = -\sin A_N / \rho_N \cos L_N$$
$$H_{12} = \cos A_N / \rho_N \cos L_N$$
$$H_{13} = H_{14} = H_{15} = H_{16} = 0$$
$$H_{21} = -\sin L_N \cos A_N / \rho_N$$
$$H_{22} = -\sin L_N \sin A_N / \rho_N$$
$$H_{23} = -\cos L_N / \rho_N$$
$$H_{24} = H_{25} = H_{26} = 0$$

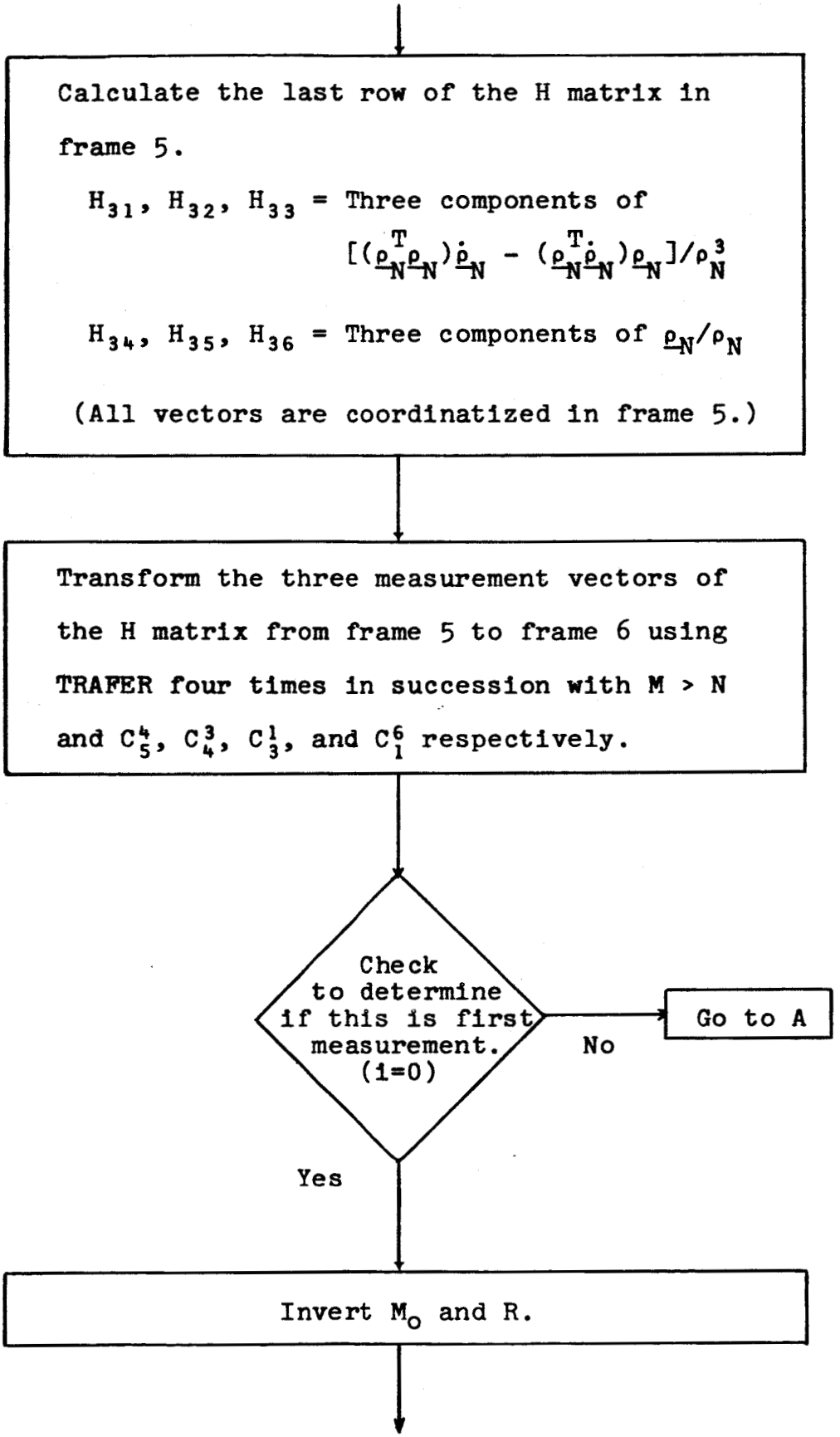
Calculate the last row of the H matrix in frame 5.
H_{31}, H_{32}, H_{33} = Three components of $[(\underline{\rho}_N^T\underline{\rho}_N)\dot{\underline{\rho}}_N - (\underline{\rho}_N^T\dot{\underline{\rho}}_N)\underline{\rho}_N]/\rho_N^3$
H_{34}, H_{35}, H_{36} = Three components of $\underline{\rho}_N/\rho_N$
(All vectors are coordinatized in frame 5.)
Transform the three measurement vectors of the H matrix from frame 5 to frame 6 using TRAFER four times in succession with M > N and C_5^4, C_4^3, C_3^1, and C_1^6 respectively.
Check to determine if this is first measurement. (i=0)
No
Go to A
Yes
Invert M_o and R.

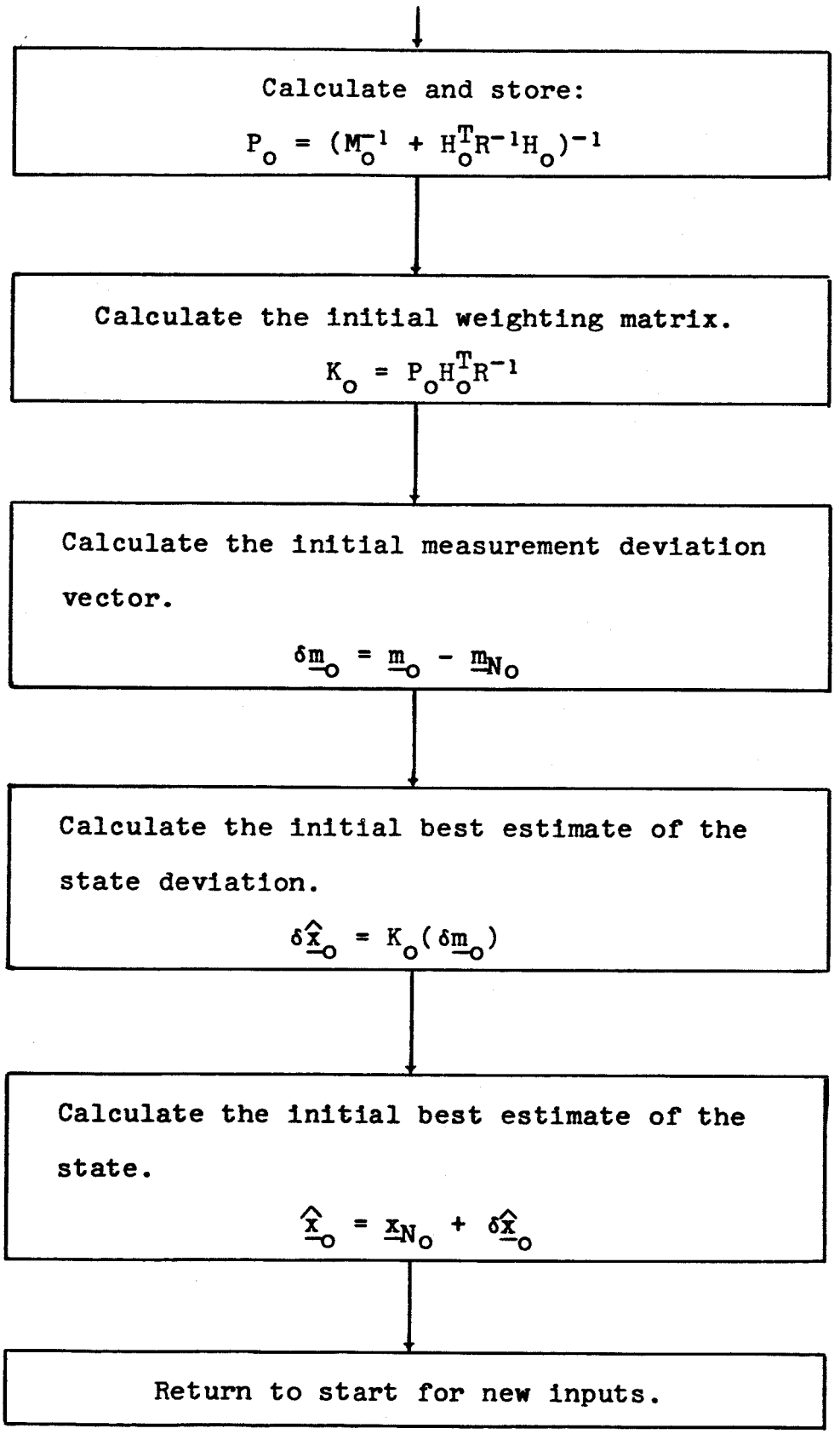
Calculate and store:
$P_o = (M_o^{-1} + H_o^T R^{-1} H_o)^{-1}$
Calculate the initial weighting matrix.
$K_o = P_o H_o^T R^{-1}$
Calculate the initial measurement deviation vector.
$\delta \underline{m}_o = \underline{m}_o - \underline{m}_{N_o}$
Calculate the initial best estimate of the state deviation.
$\delta \hat{\underline{x}}_o = K_o(\delta \underline{m}_o)$
Calculate the initial best estimate of the state.
$\hat{\underline{x}}_o = \underline{x}_{N_o} + \delta \hat{\underline{x}}_o$
Return to start for new inputs.

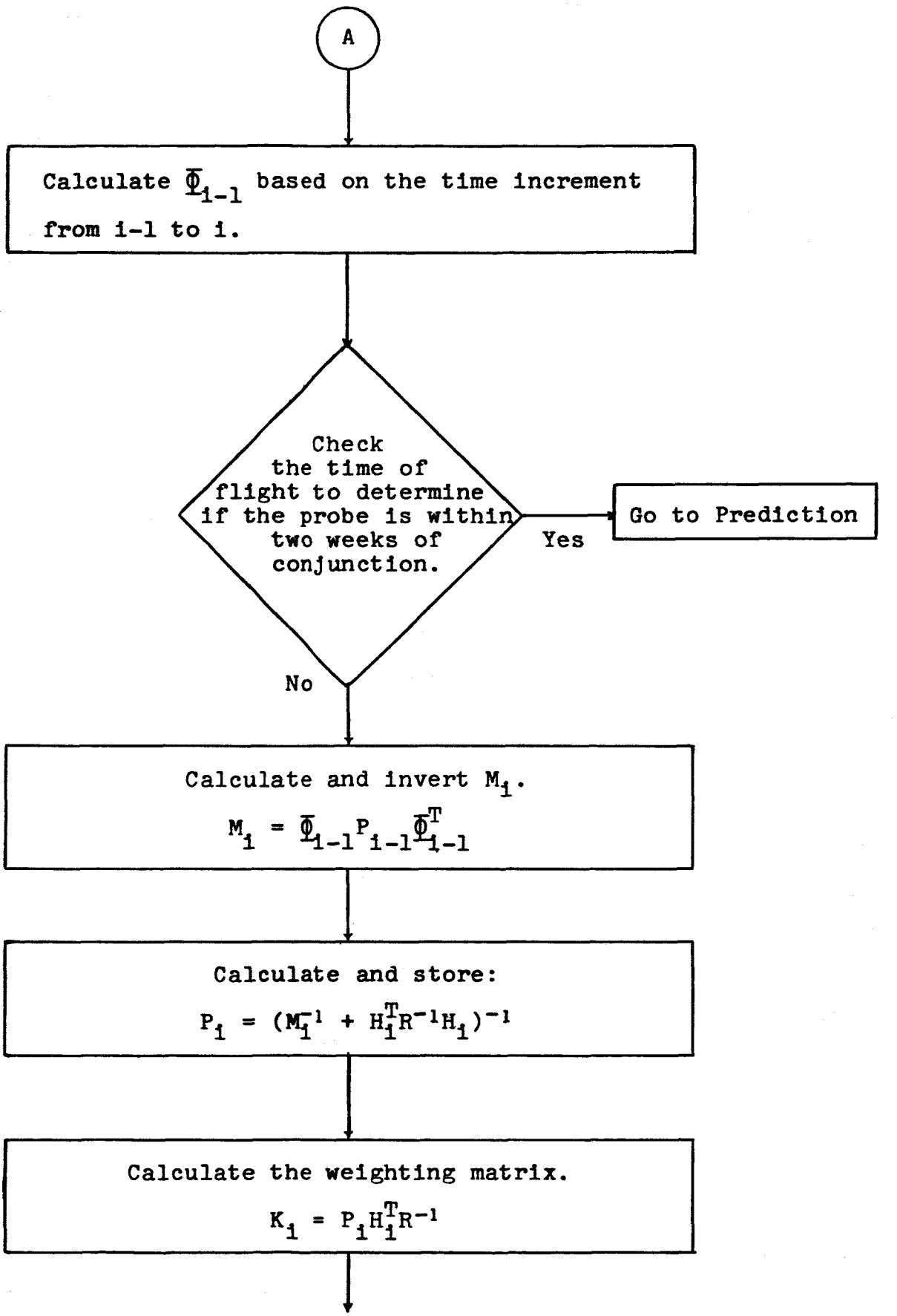
A
Calculate $\bar{\Phi}_{i-1}$ based on the time increment from i-1 to i.
Check the time of flight to determine if the probe is within two weeks of conjunction.
Yes
Go to Prediction
No
Calculate and invert M_i.
$M_i = \bar{\Phi}_{i-1} P_{i-1} \bar{\Phi}_{i-1}^T$
Calculate and store:
$P_i = (M_i^{-1} + H_i^T R^{-1} H_i)^{-1}$
Calculate the weighting matrix.
$K_i = P_i H_i^T R^{-1}$

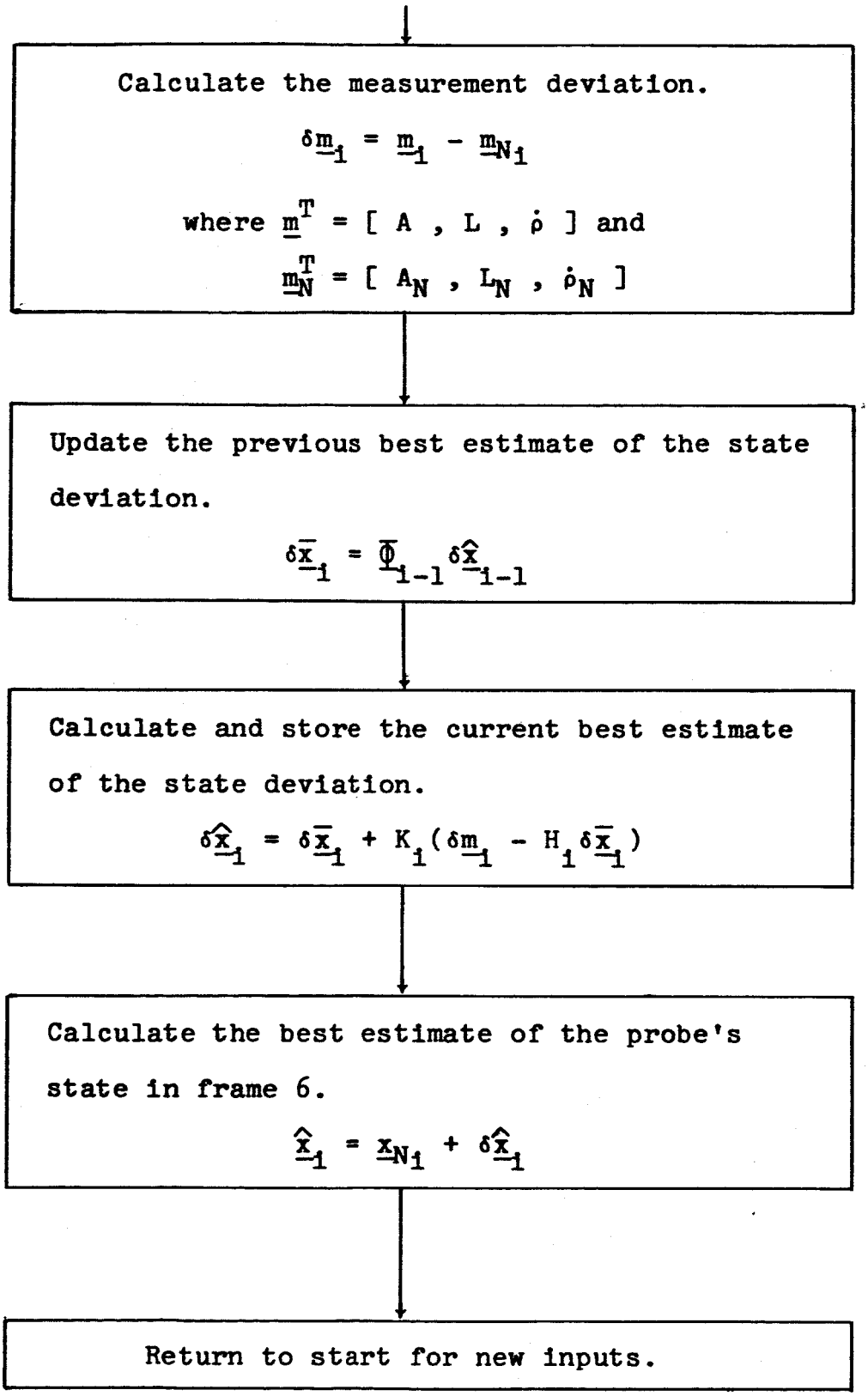
Calculate the measurement deviation.
$\delta \underline{m}_i = \underline{m}_i - \underline{m}_{N_i}$
where $\underline{m}^T = [\ A\ ,\ L\ ,\ \dot{\rho}\ ]$ and
$\underline{m}_N^T = [\ A_N\ ,\ L_N\ ,\ \dot{\rho}_N\ ]$
Update the previous best estimate of the state deviation.
$\delta \bar{\underline{x}}_i = \bar{\Phi}_{i-1} \delta \hat{\underline{x}}_{i-1}$
Calculate and store the current best estimate of the state deviation.
$\delta \hat{\underline{x}}_i = \delta \bar{\underline{x}}_i + K_i(\delta \underline{m}_i - H_i \delta \bar{\underline{x}}_i)$
Calculate the best estimate of the probe's state in frame 6.
$\hat{\underline{x}}_i = \underline{x}_{N_i} + \delta \hat{\underline{x}}_i$
Return to start for new inputs.

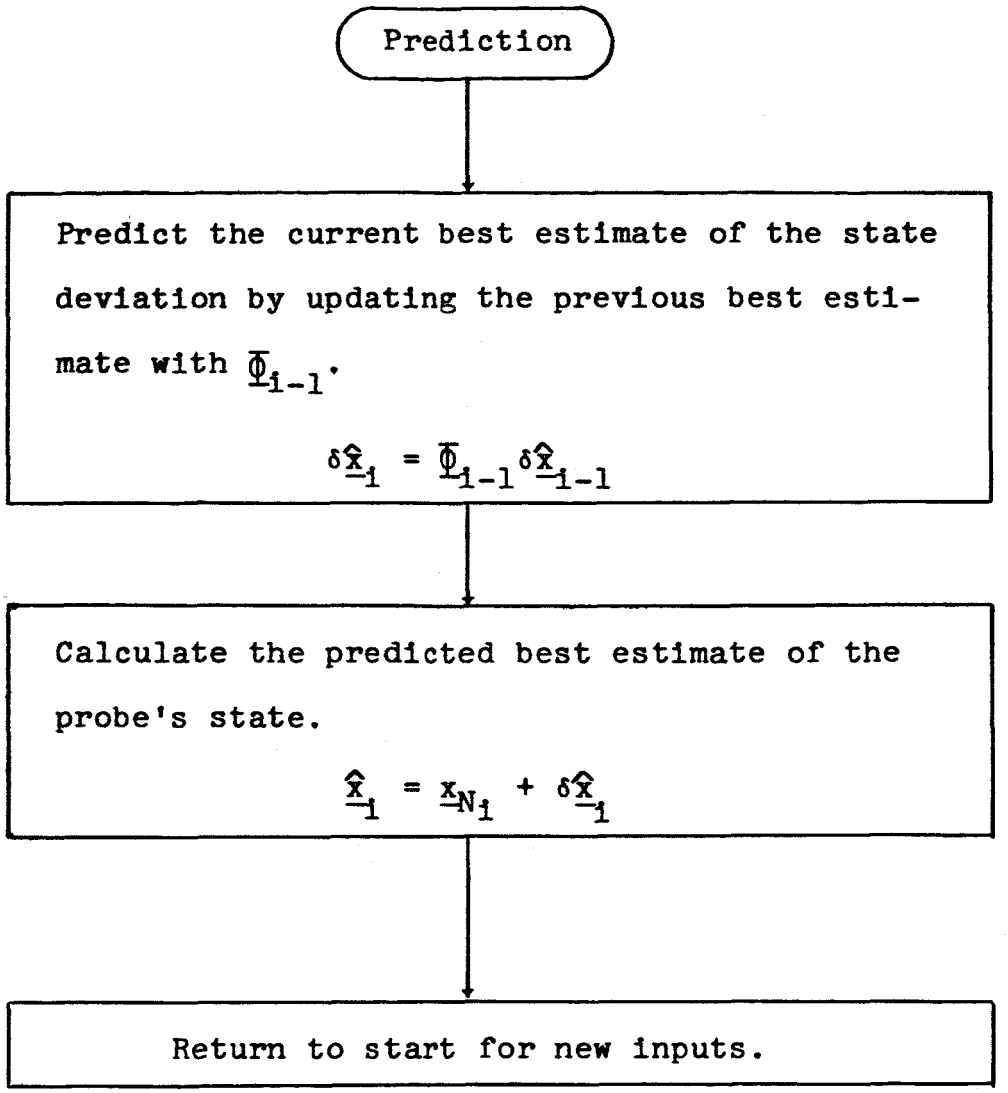
Prediction
Predict the current best estimate of the state deviation by updating the previous best estimate with $\underline{\Phi}_{i-1}$.
$\delta\hat{\underline{x}}_i = \underline{\Phi}_{i-1}\delta\hat{\underline{x}}_{i-1}$
Calculate the predicted best estimate of the probe's state.
$\hat{\underline{x}}_i = \underline{x}_{N_i} + \delta\hat{\underline{x}}_i$
Return to start for new inputs.

5.6 The Subroutines

TR1

This subroutine involves computing the elements of a transformation matrix from frame 2 to frame 1 and a transformation matrix from frame 3 to frame 2. The output of the subroutine is the matrix $C_2^1 C_3^2$ and the scalar $\delta\alpha$.

The elements of the C_2^1 matrix are representative of the luni-solar and planetary precessions of the mean equatorial plane. The computational form for the 9 elements of the matrix are as follows:

$$
\begin{aligned}
a_{11} &= 1 - .00029697T^2 - .00000013T^3 \\
a_{12} &= -a_{21} = .02234988T + .00000676T^2 \\
&\quad - .00000221T^3 \\
a_{13} &= -a_{31} = .00971711T - .00000207T^2 \\
&\quad - .00000096T^3 \\
a_{22} &= 1 - .00024976T^2 - .00000015T^3 \\
a_{23} &= a_{32} \quad -.00010859T^2 - .00000003T^3 \\
a_{33} &= 1 - .00004721T^2 + .00000002T^3
\end{aligned}
\qquad (5.1)
$$

The time T in the above expressions is the number of Julian centuries of 36,525 days past 1950.0. Theoretical discussions of the matrix elements are presented on page 66 of Reference 10 and in Reference 8. The C_2^1 matrix described here corresponds to the transpose of the A matrix outlined on pages 66 and 67 of Reference 10.

The elements of the C_3^2 matrix represent the nutation of the Earth's true equator about a mean equator and are of the

form

$$C_3^2 = \begin{bmatrix} 1 & \delta\psi\cos\bar{\varepsilon} & \delta\psi\sin\bar{\varepsilon} \\ -\delta\psi\cos\bar{\varepsilon} & 1 & \delta\varepsilon \\ -\sin\bar{\varepsilon} & -\delta\varepsilon & 1 \end{bmatrix} \qquad (5.2)$$

$\delta\psi$ denotes the nutation in longitude, while $\delta\varepsilon$ denotes the nutation in obliquity. Obliquity is the angle at which the equatorial plane is inclined to the ecliptic. $\bar{\varepsilon}$ is the mean obliquity of date.

The computational forms for $\delta\psi$, $\delta\varepsilon$, and $\bar{\varepsilon}$ are rather extensive and will not be given here. They are functions of time only and are presented on page 68 of Reference 10. $\delta\psi$ and $\delta\varepsilon$ are also carried on the JPL Ephemeris Tapes.

To complete the computation in TR1, C_3^2 is multiplied by C_2^1 to yield the desired transformation matrix C_3^1. The scalar, $\delta\alpha$, is equal to $\delta\psi\cos\bar{\varepsilon}$, one of the elements of the C_3^2 matrix.

A listing of a subroutine TR1 appears in the Appendix. This subroutine is identical to the one just described with the exception that the matrices C_1^2 and C_2^3 are computed, and the output is the matrix C_1^3, rather than C_3^1.

TR2

In TR2, the daily rotation of the Earth about its polar axis is taken into account. The routine gives either the matrix C_4^3 or its time rate of change $\dot{C}_4^3$, depending on the value of an integer N appearing in the subroutine argument list. If N is negative, C_4^3 is computed, but if N is positive, $\dot{C}_4^3$ is computed.

The matrix C_4^3 performs a simple rotation about the polar axis through the Greenwich hour angle, $\gamma(T)$, of the vernal equinox. The elements of the matrix are

$$C_4^3 = \begin{bmatrix} \cos\gamma(T) & -\sin\gamma(T) & 0 \\ \sin\gamma(T) & \cos\gamma(T) & 0 \\ 0 & 0 & 1 \end{bmatrix} \tag{5.3}$$

$\gamma(T)$ is measured from the X axis of frame 3 to the X axis of frame 4.

$$\gamma(T) = \gamma_m(T) + \delta\alpha \tag{5.4}$$

where $\delta\alpha$ is computed in TR1 and the mean value, $\gamma_m(T)$, is given in Reference 10 as

$$\gamma_m(T) = 100^\circ.07554260 + 0^\circ.9856473460d + (2^\circ.9015)10^{-13}d^2 + \omega t$$

$$0 \leq \gamma_m(T) < 360^\circ \tag{5.5}$$

T is the current epoch in UT, while d is integer days past 0^h January 1, 1950, and t is seconds past 0^h of the time T. ω, the variable Earth rotation rate, is given in Reference 10 as

$$\omega = .00417807417/(1 + (5.21)10^{-13}d) \text{ deg/sec} \tag{5.6}$$

The elements of C_4^3 are

$$\dot{C}_4^3 = \omega \begin{bmatrix} -\sin\gamma(T) & -\cos\gamma(T) & 0 \\ \cos\gamma(T) & -\sin\gamma(T) & 0 \\ 0 & 0 & 0 \end{bmatrix} \tag{5.7}$$

A listing of this subroutine is given in the Appendix.

TR3

This subroutine computes the transformation matrix from frame 5 to frame 4. The elements of C_5^4 are a function

only of geocentric latitude and longitude.

$$C_5^4 = \begin{bmatrix} -\sin\phi\cos\ell & -\sin\ell & -\cos\phi\cos\ell \\ -\sin\phi\sin\ell & \cos\ell & -\cos\phi\sin\ell \\ \cos\phi & 0 & -\sin\phi \end{bmatrix} \qquad (5.8)$$

A listing of this subroutine appears in the Appendix.

TR6

TR6 is used to compute the transformation matrix from frame 1 to frame 6, the flight path coordinate system. The computation is based on the knowledge of the three components of $\underline{R}$ and the three components of $\underline{V}$ in frame 1 plus the knowledge that the q axis of frame 6 is defined by the direction of $\underline{V}$, and the u axis is perpendicular to the plane of $\underline{R}$ and $\underline{V}$. The elements of C_1^6 are

b_{11}, b_{12}, b_{13} = Three components of $\underline{V} \times (\underline{R} \times \underline{V}) / |\underline{V} \times (\underline{R} \times \underline{V})|$

b_{21}, b_{22}, b_{23} = Three components of $\underline{V}/|\underline{V}|$

b_{31}, b_{32}, b_{33} = Three components of $\underline{R} \times \underline{V}/|\underline{R} \times \underline{V}|$ (5.9)

In the preceding expressions, $\underline{R}$ and $\underline{V}$ are coordinatized in frame 1. The transformation to frame 6 is required only because the state transition matrix was developed in that frame. A listing of TR6 appears in the Appendix.

TRAFER

This subroutine takes a 3 component column vector and multiplies it by a 3x3 matrix. The matrices used in TRAFER are the transformation matrices, C_j^k, generated by the TR subroutines. The routine will multiply the vector by either C_j^k or its transpose, which is C_k^j, since the transformation matrices are orthogonal.

If the integer M is greater than the integer N, the operation performed is

$$\underline{A}^{(k)} = C_j^k \, \underline{A}^{(j)} \tag{5.10}$$

If M < N,

$$\underline{A}^{(j)} = C_j^{k^T} \, \underline{A}^{(k)} \tag{5.11}$$

$$= C_k^j \, \underline{A}^{(k)} \tag{5.11}$$

If M = N,

$$\underline{A}^{(k)} = I\underline{A}^{(j)} \tag{5.12}$$

where I is the identity matrix and $\underline{A}$ is an arbitrary column vector that must be specified along with the transformation matrix to be used when TRAFER is called. A listing of TRAFER is given in the Appendix.

5.7 JPL Ephemeris Tapes

The JPL Ephemeris Tapes considered in this program are capable of providing the position and velocity of the planets, the Moon, and the Earth-Moon barycenter in the equatorial coordinate system of the mean equator and equinox of 1950.0 (frame 1). Planetary and Earth-Moon barycenter data are heliocentric and are expressed in AU and AU/day while the lunar data are geocentric and expressed in Earth radii and Earth radii/day. The tapes also provide the nutations and nutation rates in longitude and obliquity.

The argument of the tapes is the Julian date (ET) of the time of interest. For a discussion of the theory behind the Ephemeris Tapes, see References 8, 14, and 15.

CHAPTER 6

RESULTS AND CONCLUSIONS

To evaluate the method employed to obtain the best estimate of the probe's state, $\hat{\underline{x}}$, the state deviation error covariance matrix at conjunction, P_c, was computed. Fortunately, to compute this matrix, it is not necessary to have simulated or actual measurement data. The six diagonal elements of P_c are the standard deviations squared of the 6 components of the probe's state at conjunction in the p-q-u coordinate frame.

6.1 The Comparison

In reference 13, a similar state determination process was evaluated by D. O. Madl. From his results, he concluded that the estimation uncertainties (σ) of 4 of the 6 state components can be reduced to 20% of the value calculated without using range rate data. To achieve the 20% reduction, the uncertainty in the frequencies transmitted from the probe (σ_f) must be reduced to 1 part per 10^8 or 3/4 cycles per second. In his investigation, Madl assumed that (1) a nonrotating Earth is in a circular orbit around the Sun, (2) the tracking station is located at the center of the Earth, (3) azimuth is defined as the angle between the Earth-Sun line and the Earth-probe line, and (4) elevation, the angle

between the Earth-probe line and the ecliptic, is zero.

The results of the computation of P_c based on these assumptions are presented in Table 6.1 and shown graphically in Figures 6.1 and 6.2. The results presented in Table 6.2 and in Figures 6.3 and 6.4 were obtained by discarding these simplying assumptions and considering the complete Sun-Earth-probe system. That is, the complex motions of the Earth described in Chapter 2 were taken into account. Since the tracking station was placed on the Earth's surface, azimuth and elevation were redefined. (See section 2.2)

The numbers in Table 6.1 are very close to those in Table 6.2. This indicates that Madl's conclusions are valid even when the complete geometrical model is considered. The fact that the results do agree does not mean that the simplifying assumptions can be used in the processing of actual data. These assumptions were used to construct a simple geometric model in order to evaluate the application of Kalman filtering. In an actual data processing scheme such as SPADAF, only the complete geometrical model is valid. To illustrate this point, consider the H matrix which is based on the nominal values $\dot{\rho}_N$, A_N, and L_N. The nominal values are not the same for both models. For example, elevation is always zero in the simplified model, while in the actual situation, elevation would vary during the day as the probe appeared to move across the sky because of Earth rotation.

Although the results of this analysis verify Madl's conclusions, the numbers presented in Table 6.1 do not agree

exactly with the numbers he presented (13: 45). This disagreement is due to mistakes in the program he used to compute P_c.

6.2 Measurement Scheduling

To make a comparison between the results computed using Madl's model and those computed using the complete model, his original time schedule was changed to conform with times at which ephemeris data was available. The change in any one measurement time was not more than two days. It can be seen by comparing the data in Table 6.1 with that in Table 6.3A, that this slight change caused a 10% to 30% change in the diagonal elements of the P_c matrix.

This result suggested that some "best" schedule might exist. The measurements affect the P_c matrix by the relationship expressed in equation 4.10. By carrying out the matrix multiplication for the term $H^TR^{-1}H$, the relationship of the various elements of the H matrix to the elements of the P matrix can be seen. This relationship shows that by increasing the elements of the H matrix at each measurement time, the P_c matrix will be decreased. H is a function of A, L, $\underline{\rho}$, and $\dot{\rho}$. In the simple model L is constrained to be zero. Because azimuth varys slowly over the course of the orbit in the simple case, it has a small effect on the computation of the H matrix. Thus the simple model can be used to investigate the effect of $\underline{\rho}$ and $\dot{\rho}$ on the P_c matrix for several measurement schedules. The low range rate, high range rate, and early time data sets presented in Table 6.3B, C, and D show

TABLE 6.1

Position and Velocity Uncertainties for Selected Range-Rate Standard Deviations Calculated Using Simplified Model

$\sigma_{\dot{\rho}}$ m/sec σ_f cps	σ_{Rp} AU Km	σ_{Rq} AU Km	σ_{Ru} AU Km	σ_{Vp} AU/yr Km/sec	σ_{Vq} AU/yr Km/sec	σ_{Vu} AU/yr Km/sec
300	$.1439\ 10^{-3}$	$.8223\ 10^{-3}$	$.3498\ 10^{-4}$	$.1021\ 10^{-1}$	$.1846\ 10^{-2}$	$.2745\ 10^{-2}$
75	21,530	123,017	5233	$.484\ 10^{-1}$	$.875\ 10^{-2}$	$.1301\ 10^{-1}$
200	$.1428\ 10^{-3}$	$.8013\ 10^{-3}$	same	$.9963\ 10^{-2}$	$.1831\ 10^{-2}$	same
50	21,364	119,877		$.472\ 10^{-1}$	$.867\ 10^{-2}$	
100	$.1374\ 10^{-3}$	$.7108\ 10^{-3}$	same	$.8884\ 10^{-2}$	$.1760\ 10^{-2}$	same
25	20,562	106,333		$.421\ 10^{-1}$	$.834\ 10^{-2}$	
60	$.1273\ 10^{-3}$	$.5805\ 10^{-3}$	same	$.7328\ 10^{-2}$	$.1628\ 10^{-2}$	same
15	19,046	86,842		$.347\ 10^{-1}$	$.772\ 10^{-2}$	
30	$.9975\ 10^{-4}$	$.3649\ 10^{-3}$	same	$.4722\ 10^{-2}$	$.1273\ 10^{-2}$	same
7.5	14,922	54,591		$.224\ 10^{-1}$	$.603\ 10^{-2}$	
10	$.4556\ 10^{-4}$	$.1352\ 10^{-3}$	same	$.1826\ 10^{-2}$	$.5845\ 10^{-3}$	same
2.5	6,816	20,234		$.866\ 10^{-2}$	$.277\ 10^{-2}$	
3	$.1492\ 10^{-4}$	$.4155\ 10^{-4}$	same	$.5772\ 10^{-3}$	$.1968\ 10^{-3}$	same
0.75	2,231	6,215		$.273\ 10^{-2}$	$.933\ 10^{-3}$	
0.6	$.3028\ 10^{-5}$	$.8345\ 10^{-5}$	same	$.1167\ 10^{-3}$	$.4034\ 10^{-4}$	same
0.15	453	1,248		$.553\ 10^{-3}$	$.191\ 10^{-3}$	

Table 6.1, continued

$\sigma_{\dot{\rho}}$ m/sec σ_f cps	σ_{Rp} AU Km	σ_{Rq} AU Km	σ_{Ru} AU Km	σ_{Vp} AU/yr Km/sec	σ_{Vq} AU/yr Km/sec	σ_{Vu} AU/yr Km/sec
0.3	$.1515\ 10^{-5}$	$.4173\ 10^{-5}$	same	$.5839\ 10^{-4}$	$.2019\ 10^{-4}$	same
0.075	226	624		$.277\ 10^{-3}$	$.957\ 10^{-4}$	
0.06	$.3030\ 10^{-6}$	$.8347\ 10^{-6}$	same	$.1168\ 10^{-4}$	$.4039\ 10^{-5}$	same
0.015	45	125		$.554\ 10^{-4}$	$.191\ 10^{-4}$	
0.03	$.1515\ 10^{-6}$	$.4173\ 10^{-6}$	same	$.5840\ 10^{-5}$	$.2020\ 10^{-5}$	same
0.0075	23	62		$.277\ 10^{-4}$	$.957\ 10^{-5}$	
Angle data degraded to $\sigma^2 = 1°$						
0.6	$.303\ 10^{-5}$	$.8347\ 10^{-5}$	$.1540\ 10^{-3}$	$.1168\ 10^{-3}$	$.4039\ 10^{-4}$	$.1932\ 10^{-1}$
0.15	453	1,249	23,033	$.554\ 10^{-3}$	$.191\ 10^{-3}$	$.9157\ 10^{-1}$

Note: All frequency uncertainties in this table and in the following tables and graphs are based on a 75 Mc carrier frequency.

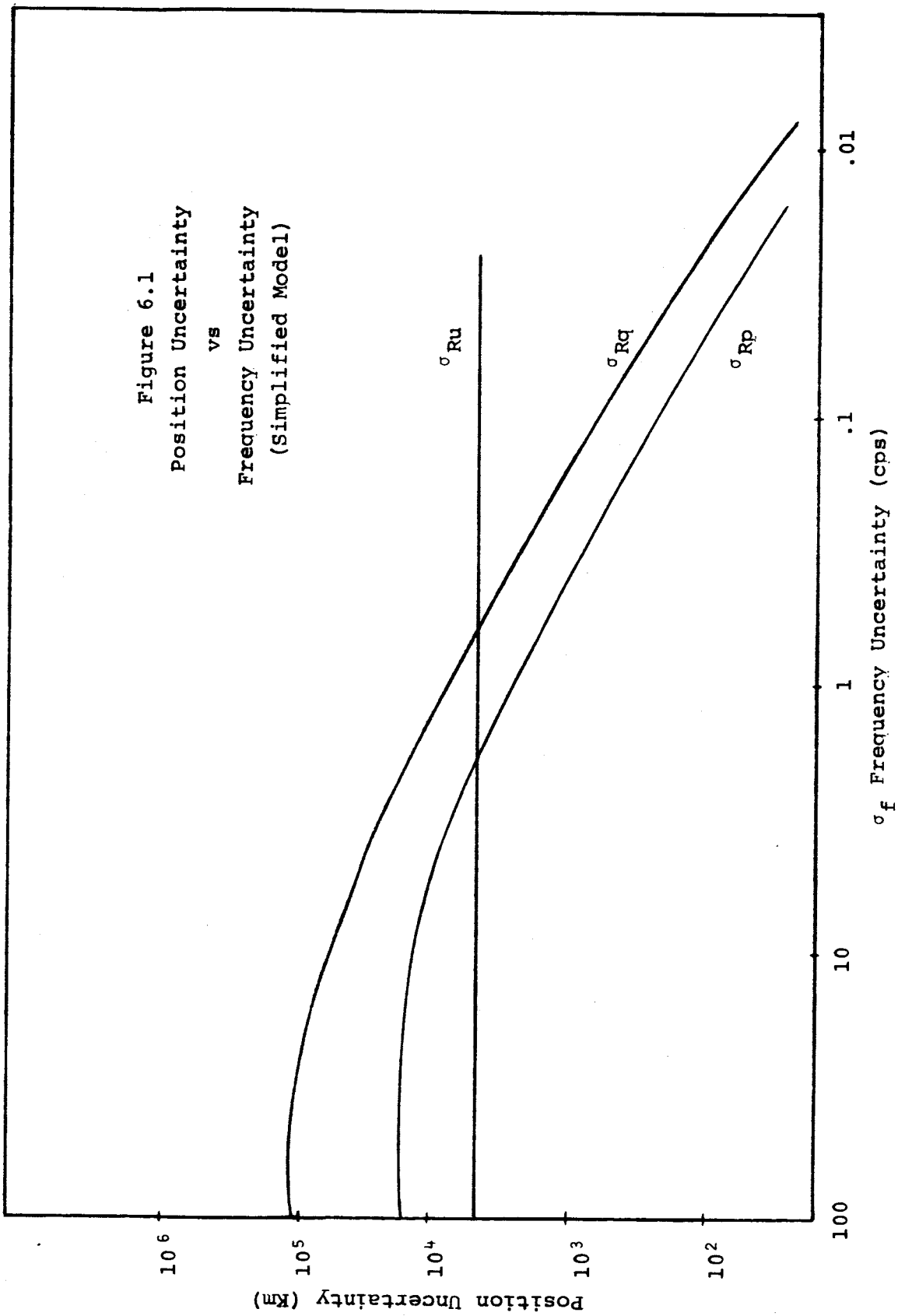

Figure 6.1
Position Uncertainty
vs
Frequency Uncertainty
(Simplified Model)

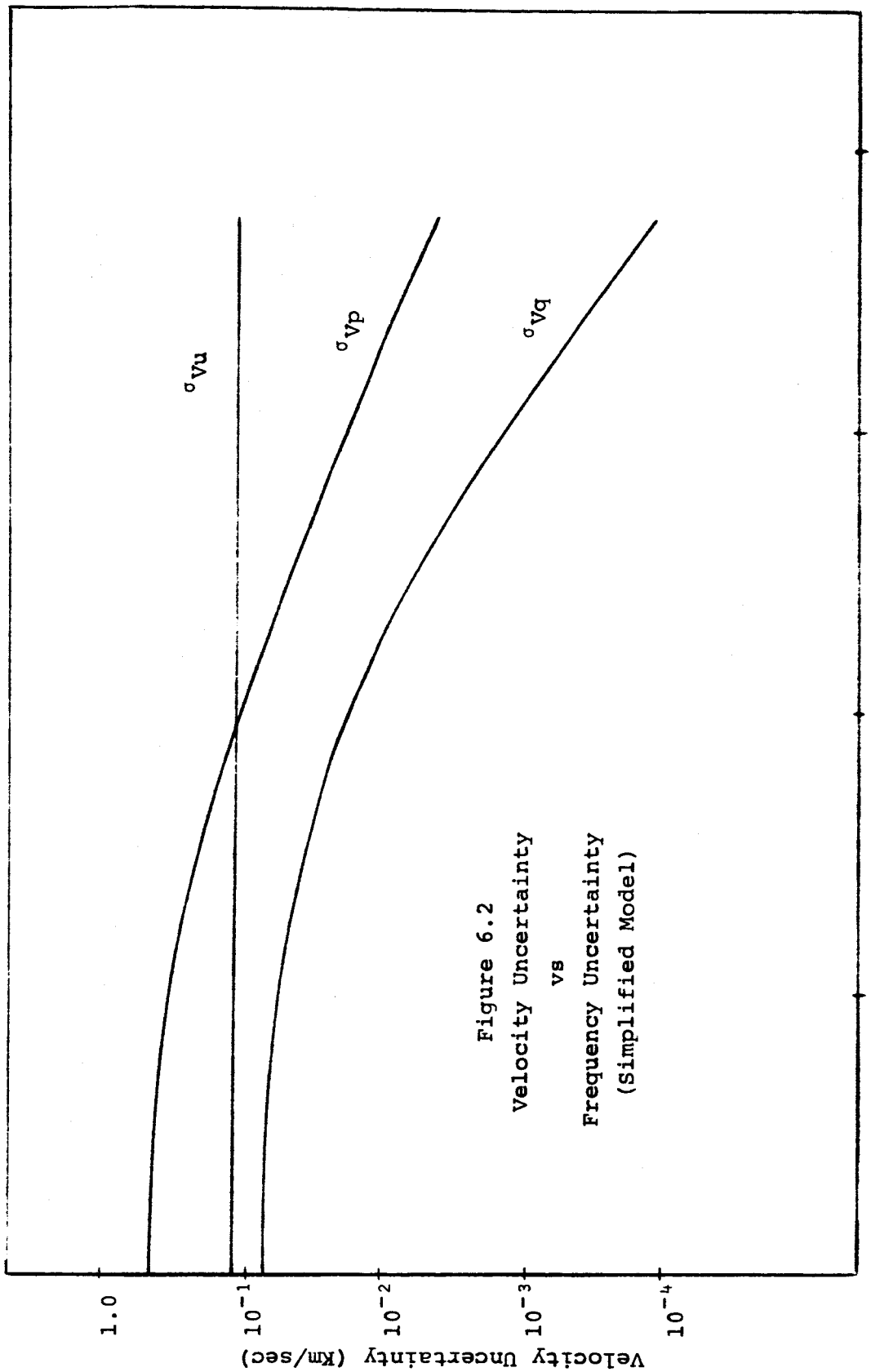

Figure 6.2
Velocity Uncertainty
vs
Frequency Uncertainty
(Simplified Model)

TABLE 6.2

Position and Velocity Uncertainties for Selected Range-Rate Standard Deviations
Calculated Using Complete Model

$\sigma_{\dot{\rho}}$ m/sec σ_f cps	σ_{Rp} AU Km	σ_{Rq} AU Km	σ_{Ru} AU Km	σ_{Vp} AU/yr Km/sec	σ_{Vq} AU/yr Km/sec	σ_{Vu} AU/yr Km/sec
300	$.1453\ 10^{-3}$	$.9618\ 10^{-3}$	$.2736\ 10^{-4}$	$.1216\ 10^{-1}$	$.1927\ 10^{-2}$	$.2570\ 10^{-2}$
75	21,700	144,000	4,092	$.576\ 10^{-1}$	$.914\ 10^{-2}$	$.1218\ 10^{-1}$
200	$.1435\ 10^{-3}$	$.9310\ 10^{-3}$	$.2736\ 10^{-4}$	$.1178\ 10^{-1}$	$.1898\ 10^{-2}$	$.2570\ 10^{-2}$
50	21,460	139,270	4,092	$.558\ 10^{-1}$	$.900\ 10^{-2}$	$.1218\ 10^{-1}$
100	$.1352\ 10^{-3}$	$.7971\ 10^{-3}$	$.2735\ 10^{-4}$	$.1012\ 10^{-1}$	$.1770\ 10^{-2}$	$.2570\ 10^{-2}$
25	20,226	119,250	4,092	$.470\ 10^{-1}$	$.839\ 10^{-2}$	$.1218\ 10^{-1}$
60	$.1230\ 10^{-3}$	$.6268\ 10^{-3}$	$.2735\ 10^{-4}$	$.8004\ 10^{-2}$	$.1591\ 10^{-2}$	$.2570\ 10^{-2}$
15	18,397	93,763	4,092	$.379\ 10^{-2}$	$.754\ 10^{-2}$	$.1218\ 10^{-1}$
30	$.9599\ 10^{-4}$	$.3769\ 10^{-3}$	$.2735\ 10^{-4}$	$.4895\ 10^{-2}$	$.1229\ 10^{-2}$	$.2568\ 10^{-2}$
7.5	14,360	56,385	4,092	$.232\ 10^{-1}$	$.582\ 10^{-2}$	$.1217\ 10^{-1}$
10	$.4469\ 10^{-4}$	$.1376\ 10^{-3}$	$.2734\ 10^{-4}$	$.1848\ 10^{-2}$	$.5833\ 10^{-3}$	$.2563\ 10^{-2}$
2.5	6,685	20,585	4,090	$.876\ 10^{-2}$	$.277\ 10^{-2}$	$.1215\ 10^{-1}$
3	$.1468\ 10^{-4}$	$.4256\ 10^{-4}$	$.2731\ 10^{-4}$	$.5836\ 10^{-3}$	$.1970\ 10^{-3}$	$.2557\ 10^{-2}$
0.75	2,196	6,367	4,087	$.277\ 10^{-2}$	$.934\ 10^{-3}$	$.1212\ 10^{-1}$
0.6	$.2979\ 10^{-5}$	$.8580\ 10^{-5}$	$.2700\ 10^{-4}$	$.1182\ 10^{-3}$	$.4018\ 10^{-4}$	$.2502\ 10^{-2}$
0.15	446	1,284	4,039	$.560\ 10^{-3}$	$.190\ 10^{-3}$	$.1176\ 10^{-1}$

Table 6.2, continued

σ_ρ m/sec σ_f cps	σ_{Rp} AU Km	σ_{Rq} AU Km	σ_{Ru} AU Km	σ_{Vp} AU/yr Km/sec	σ_{Vq} AU/yr Km/sec	σ_{Vu} AU/yr Km/sec
0.3	$.1491\ 10^{-5}$	$.4319\ 10^{-5}$	$.2614\ 10^{-4}$	$.5960\ 10^{-4}$	$.2012\ 10^{-4}$	$.2356\ 10^{-2}$
0.075	223	646	3,910	$.283\ 10^{-3}$	$.954\ 10^{-4}$	$.1117\ 10^{-1}$
0.06	$.3006\ 10^{-6}$	$.9086\ 10^{-6}$	$.1710\ 10^{-4}$	$.1284\ 10^{-4}$	$.4078\ 10^{-5}$	$.1136\ 10^{-2}$
0.015	45	136	2,557	$.609\ 10^{-4}$	$.193\ 10^{-4}$	$.5386\ 10^{-2}$
0.03	$.1509\ 10^{-6}$	$.4637\ 10^{-6}$	$.1079\ 10^{-4}$	$.6652\ 10^{-5}$	$.2057\ 10^{-5}$	$.6340\ 10^{-3}$
0.0075	23	69	1,615	$.315\ 10^{-4}$	$.975\ 10^{-5}$	$.3006\ 10^{-2}$
Angle data degraded to $\sigma^2 = 1°$						
0.6	$.2994\ 10^{-5}$	$.8871\ 10^{-5}$	$.1212\ 10^{-3}$	$.1236\ 10^{-3}$	$.4049\ 10^{-4}$	$.9484\ 10^{-2}$
0.15	448	1,327	18,129	$.586\ 10^{-3}$	$.192\ 10^{-3}$	$.4496\ 10^{-1}$

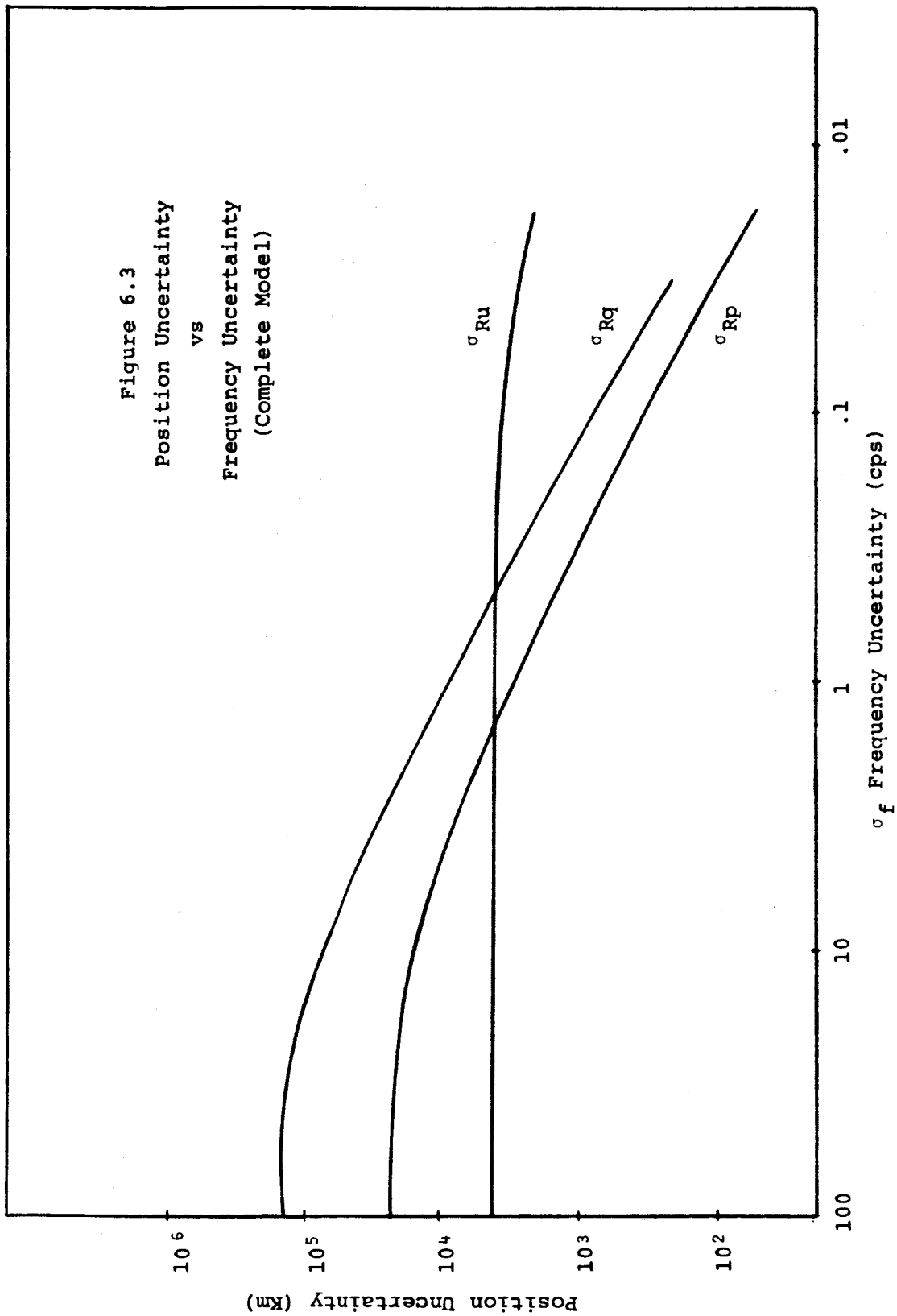
Figure 6.3
Position Uncertainty
vs
Frequency Uncertainty
(Complete Model)
σ_{Ru}
σ_{Rq}
σ_{Rp}
Position Uncertainty (Km)
10^6
10^5
10^4
10^3
10^2
100
10
1
.1
.01
σ_f Frequency Uncertainty (cps)

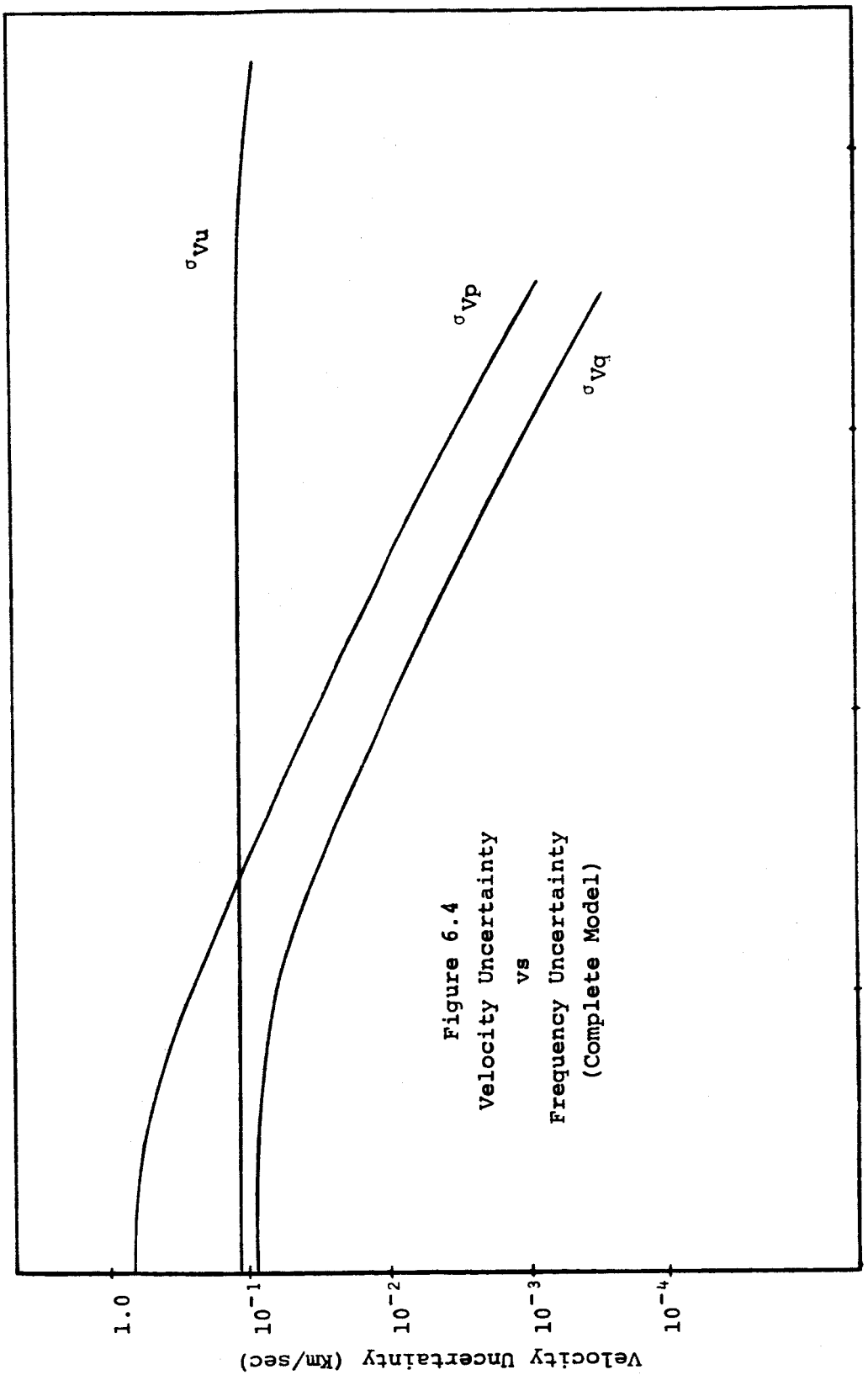

Figure 6.4
Velocity Uncertainty
vs
Frequency Uncertainty
(Complete Model)

the wide variation in P_c for different schedules.

First, it is interesting to compare the out-of-plane components for the three schedules. Since range rate does not affect the out-of-plane component in the simplified model, the out-of-plane standard deviations are the same for all σ_f's.

Low Range Rate	σ_{Ru}	= 3614	Km
	σ_{Vu}	= .00914	Km/sec
High Range Rate	σ_{Ru}	= 4507	Km
	σ_{Vu}	= .0178	Km/sec
Early Times	σ_{Ru}	= 1627	Km
	σ_{Vu}	= .0116	Km/sec

The position deviation for the Early Time group is by far the smallest. This is reasonable for the early times were grouped when range had its smallest value. $\frac{1}{\rho}$ is the only element of the H matrix that enters in the computation of the σ_{Ru} element of P_c. If ρ is small, $\frac{1}{\rho}$ will be large, and P_c should be decreased. The velocity components are affected by the position deviation through the state transition matrix. A reasonable explanation for the differences in these velocity variations is obscured by the complex mathematical relationships.

Next the in-plane components will be compared for two frequency variations. First when σ_f = 75 cps,

Low Range Rate	σ_{Rp}	= 19,607	Km

σ_{Rq} = 108,695 Km

σ_{Vp} = .0419 Km/sec

σ_{Vq} = .00793 Km/sec

High Range Rate σ_{Rp} = 23,135 Km

σ_{Rq} = 144,105 Km

σ_{Vp} = .0564 Km/sec

σ_{Vq} = .00929 Km/sec

Early Times σ_{Rp} = 28,538 Km

σ_{Rq} = 132,636 Km

σ_{Vp} = .0536 Km/sec

σ_{Vq} = .0114 Km/sec

σ_f = .75 cps

Low Range Rate σ_{Rp} = 3127 Km

σ_{Rq} = 10,426 Km

σ_{Vp} = .00444 Km/sec

σ_{Vq} = .00131 Km/sec

High Range Rate σ_{Rp} = 1716 Km

σ_{Rq} = 6135 Km

σ_{Vp} = .00308 Km/sec

σ_{Vq} = .000687 Km/sec

Early Times σ_{Rp} = 3012 Km

σ_{Rq} = 9608 Km

σ_{Vp} = .00394 Km/sec

σ_{Vq} = .00119 Km/sec

The in-plane components are functions of A, $\underline{\rho}$ and $\dot{\rho}$. When knowledge of the range rate is not good, the low range rate schedule produces smaller in-plane variations.

TABLE 6.3

Position and Velocity Uncertainties for Selected Range-Rate Standard Deviations Using Several Time Schedules

$\sigma_{\dot{\rho}}$ m/sec σ_f cps	σ_{Rp} AU Km	σ_{Rq} AU Km	σ_{Ru} AU Km	σ_{Vp} AU/yr Km/sec	σ_{Vq} AU/yr Km/sec	σ_{Vu} AU/yr Km/sec
A. Madl's Times (Simplified Model)						
300	$.1431\ 10^{-3}$	$.7903\ 10^{-3}$	$.2628\ 10^{-4}$	$.9817\ 10^{-2}$	$.1822\ 10^{-2}$	$.2613\ 10^{-2}$
75	21,407	118,228	3,932	$.465\ 10^{-1}$	$.864\ 10^{-2}$	$.124\ 10^{-1}$
30	$.1004\ 10^{-3}$	$.3659\ 10^{-3}$	same	$.4744\ 10^{-2}$	$.1275\ 10^{-2}$	same
7.5	15,025	54,746		$.225\ 10^{-1}$	$.604\ 10^{-2}$	
3	$.1494\ 10^{-4}$	$.4216\ 10^{-4}$	same	$.5862\ 10^{-3}$	$.1946\ 10^{-3}$	same
0.75	2,236	6,308		$.278\ 10^{-2}$	$.923\ 10^{-3}$	
B. Early Time Group (Simplified Model)						
300	$.1908\ 10^{-3}$	$.8866\ 10^{-3}$	$.1087\ 10^{-4}$	$.1131\ 10^{-1}$	$.2413\ 10^{-2}$	$.2449\ 10^{-2}$
75	28,538	132,636	1,627	$.536\ 10^{-1}$	$.114\ 10^{-1}$	$.116\ 10^{-1}$
30	$.1333\ 10^{-3}$	$.5197\ 10^{-3}$	same	$.6691\ 10^{-2}$	$.1683\ 10^{-2}$	same
7.5	19,946	77,751		$.317\ 10^{-1}$	$.798\ 10^{-2}$	
3	$.2013\ 10^{-4}$	$.6423\ 10^{-4}$	same	$.8306\ 10^{-3}$	$.2520\ 10^{-3}$	same
0.75	3,012	9,608		$.394\ 10^{-2}$	$.119\ 10^{-2}$	
C. High Range-Rate Time Group (Simplified Model)						
300	$.1546\ 10^{-3}$	$.9632\ 10^{-3}$	$.3013\ 10^{-4}$	$.1190\ 10^{-1}$	$.1959\ 10^{-2}$	$.3757\ 10^{-2}$
75	23,135	144,105	4,507	$.564\ 10^{-1}$	$.929\ 10^{-2}$	$.178\ 10^{-1}$

Table 6.3, continued

$\sigma_{\dot{\rho}}$ m/sec σ_f cps	σ_{Rp} AU Km	σ_{Rq} AU Km	σ_{Ru} AU Km	σ_{Vp} AU/yr Km/sec	σ_{Vq} AU/yr Km/sec	σ_{Vu} AU/yr Km/sec
30	$.8780\ 10^{-4}$	$.3504\ 10^{-3}$	same	$.4554\ 10^{-2}$	$.1109\ 10^{-2}$	same
7.5	13,135	52,425		$.216\ 10^{-1}$	$.526\ 10^{-2}$	
3	$.1147\ 10^{-4}$	$.4101\ 10^{-4}$	same	$.6497\ 10^{-3}$	$.1449\ 10^{-3}$	same
0.75	1,716	6,135		$.308\ 10^{-2}$	$.687\ 10^{-3}$	
D. Low Range-Rate Time Group (Simplified Model)						
300	$.1311\ 10^{-3}$	$.7266\ 10^{-3}$	$.2416\ 10^{-4}$	$.8841\ 10^{-2}$	$.1673\ 10^{-2}$	$.1928\ 10^{-2}$
75	19,607	108,695	3,614	$.419\ 10^{-1}$	$.793\ 10^{-2}$	$.914\ 10^{-2}$
30	$.1061\ 10^{-3}$	$.4751\ 10^{-3}$	same	$.6088\ 10^{-2}$	$.1355\ 10^{-2}$	same
7.5	15,866	71,082		$.289\ 10^{-1}$	$.642\ 10^{-2}$	
3	$.2090\ 10^{-4}$	$.6970\ 10^{-4}$	same	$.9372\ 10^{-3}$	$.2761\ 10^{-3}$	same
0.75	3,127	10,426		$.444\ 10^{-2}$	$.131\ 10^{-2}$	
E. Times Used for Tables 6.1 and 6.2 + 6 Hours (Complete Model)						
300	$.1200\ 10^{-3}$	$.7734\ 10^{-3}$	$.2047\ 10^{-4}$	$.9806\ 10^{-4}$	$.1636\ 10^{-2}$	$.2126\ 10^{-2}$
75	17,900	115,300	3,060	$.465\ 10^{-3}$	$.775\ 10^{-2}$	$.997\ 10^{-2}$
30	$.8047\ 10^{-4}$	$.3617\ 10^{-3}$	$.2012\ 10^{-4}$	$.4656\ 10^{-2}$	$.1055\ 10^{-2}$	$.2083\ 10^{-2}$
7.5	12,550	53,900	3,022	$.221\ 10^{-1}$	$.500\ 10^{-2}$	$.998\ 10^{-2}$
3	$.1461\ 10^{-4}$	$.4302\ 10^{-4}$	$.1855\ 10^{-4}$	$.5921\ 10^{-3}$	$.1948\ 10^{-3}$	$.2058\ 10^{-2}$
0.75	2,190	6,430	2,775	$.2805\ 10^{-2}$	$.922\ 10^{-3}$	$.974\ 10^{-2}$

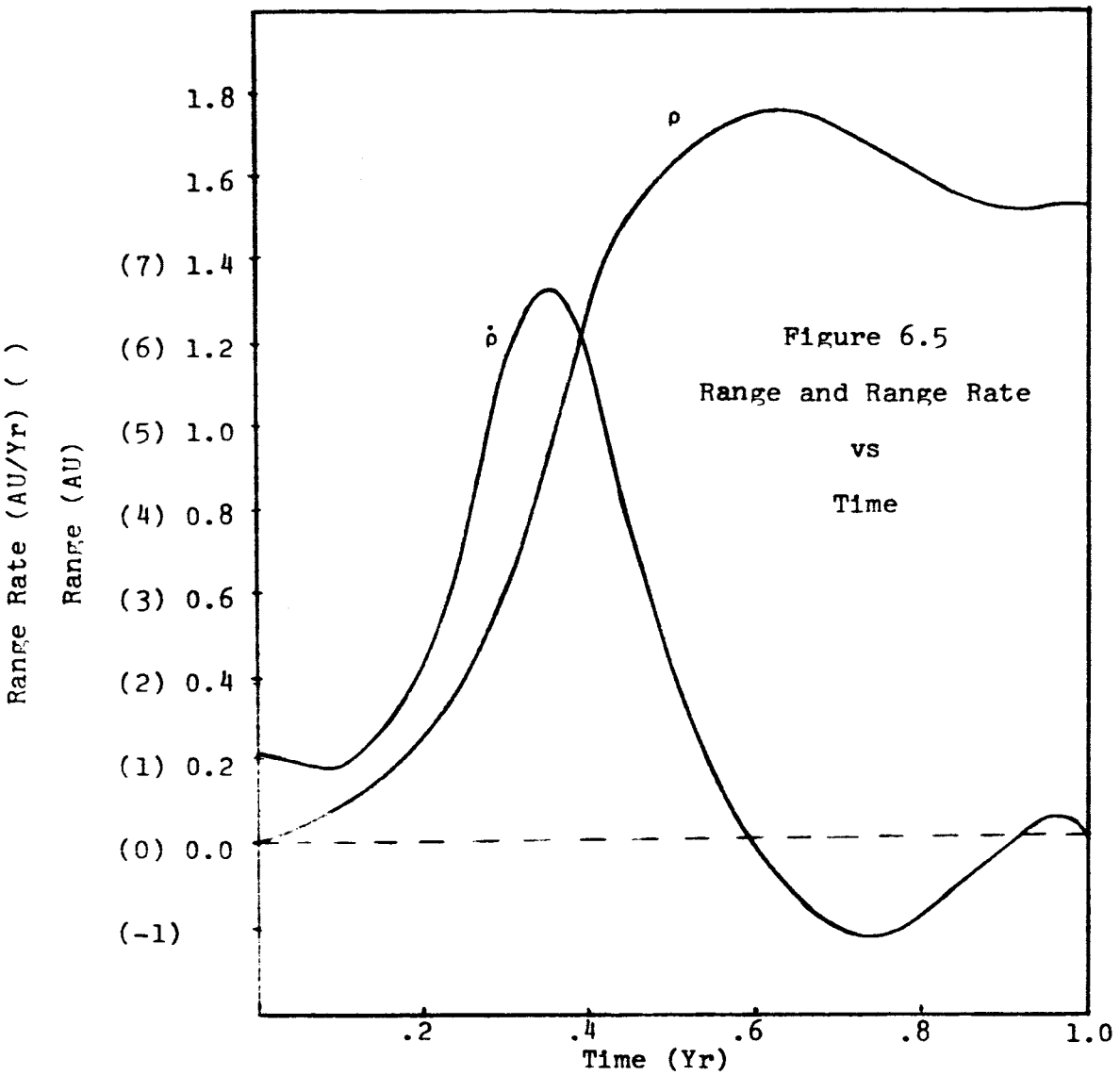

Figure 6.5

Range and Range Rate

vs

Time

Measurement Schedules

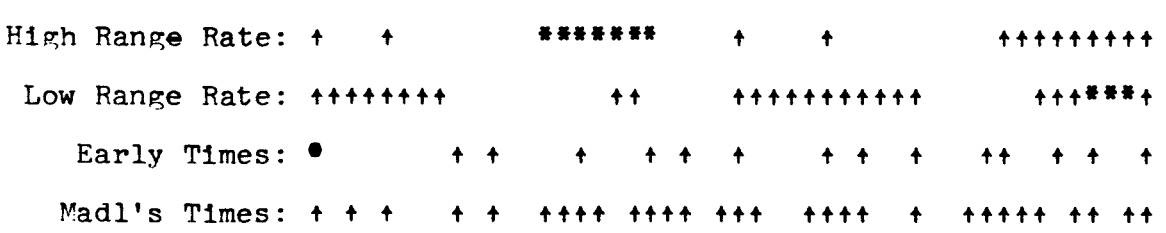

● indicates clustered measurements

However, when the quality of the range rate information improves considerably, the high range rate schedule determines better in-plane components.

The various schedules used indicate that while some "best" mission schedule does exist, it is not just a simple function of the measurement variables. The quality of the measurements and the state transition matrix must also be considered.

In the actual data processing situation, the problem may be examined in two parts. The first is the mission scheduling phase which is the same as that illustrated by the simple model. That is, since $\underline{\rho}$ and $\dot{\rho}$ vary slowly, the measurements should be scheduled over the course of the mission with the values of $\underline{\rho}$ and $\dot{\rho}$ in mind. Next a daily time schedule could be worked out in light of the large diurnal variation of azimuth and elevation caused by the Earth's rotation. (Their values are constrained by the viewability of the probe from the station and by the Earth-probe position relationship.) Since $\underline{\rho}$ and $\dot{\rho}$ do not vary a great deal during the course of a day, changing all the times by six hours would allow the effect of azimuth and elevation to be studied. The data presented in Table 6.3E can be compared to the data in Table 6.2. For just a six hour change in all the measurement times, the elements of the P_c matrix differ by as much as 30%. This would suggest that some "best" daily schedule does exist.

The effect of the H matrix is not the only factor that must be considered in the actual case. The fact that

atmospheric refraction has a greater effect when the elevation angle is small might restrict the allowable measurement times. Also, there might be physical restrictions on the pointing of the antennas. A possible extension of this thesis would be to examine the scheduling problem in depth, including the mathematical maximization problem as well as practical considerations.

APPENDIX

THE COMPUTER PROGRAMS FOR P_c

The object of this appendix is to describe the two computer programs used to calculate the state deviation error covariance matrix at conjunction, P_c. Both programs are written in Fortran IV for use on the IBM System 360.

A.1 Madl's Program

The first program utlizes a main program and a subroutine VCTR based on Madl's simplified model of the Sun-Earth-probe system outlined in Chapter 6.

The inputs for this program are the measurement times, ST(I), in years past launch; the three measurement variances, SS(J), in rad^2 and AU^2/Yr^2; and the 6 elements of the initial error covariance matrix, EO(K,K), in AU^2 and AU^2/Yr^2.(13:48) Other variables in the program are as follows:

AM semi-major axis of the nominal probe trajectory

U Sun's gravitational constant

E nominal probe orbit eccentricity

AVN mean angular motion of the probe

AI eccentric anomaly of the probe's initial point

A listing of the main program and the 17 subroutines used is presented in A.4. The subroutine VCTR computes the 18

elements of the H matrix while the TR6 and TRAFER routines deal with vector transformations and are described in Chapter 5. KEPLER is based on Battin's universal formulae for conic orbits.(2:49) When the vector components of the initial position and velocity of a body are specified in a coordinate frame, KEPLER computes the components of position and velocity in the same frame at some specified later time. Two body mechanics are assumed.

The remaining 13 subroutines, XTRP, TRUE, CCOM, PERI, NVRT, MTRM, MTRN, MTRS, MTRT, MPY1, MPY2, MPY3, and SUM, were written by Mr. John Fagan and are discussed briefly in Reference 13. Basically, Fagan's routines calculate a two body state transition matrix in frame 6 and use that matrix to continually update best estimates of P which are based on the H, R, and M matrices.

A.2 The Geometrically Exact Program

This program utilizes a main program and a subroutine VCTR based on the actual motions of the Earth in inertial space. The program listing presented in A.5 contains the main program and the subroutines VCTR, TR1, TR2, and TR3. These last three subroutines were explained in Chapter 5. Although not contained in the listing, this program uses the subroutines TR6, TRAFER, KEPLER, and Fagan's 13 subroutines which were mentioned in the preceding section.

The inputs to the program include the inputs mentioned in A.1 plus tabular values for the position and velocity of the Earth with respect to the Sun in a heliocentric mean

ecliptic and equinox coordinate system of 1950.0 and the position and velocity of the Moon with respect to the Earth in a geocentric mean ecliptic and equinox coordinate system of 1950.0. These positions and velocities are rotated through the angle $\bar{\epsilon}$ to frame 1. Normally, if the JPL Ephemeris Tapes are used rather than tabular values, a rotation is not necessary because the positions and velocities are available in frame 1.

A.3 General Comments

The components of the probe's initial position and velocity vectors in frame 1 are specified in the main program (RIL and VIL). These components are based on the orbit parameters given in Chapter 1.

The measurement times used to compute the values listed in Tables 6.1 and 6.2 are spaced over the period of one year to coincide with the occurrences of high range rate. With the exception of the ephemeris data, the inputs to both programs are identical and are listed in A.4.

Again, it is important to note that it is not necessary to have actual measurement data to obtain the final result, P at conjunction.

A.4 Listing of Madl's Program (Corrected)

```
      COMMON   U,CV,TL,BB,RME(30,3),VME(30,3),RBS(30,3),VBS(30,3),
     1TR45(3,3),RIL(3),VIL(3),R4(3),ST(30),EX(6,6),SS(3),E,AVN,EAC,F,PI,
     2AM
      DOUBLE PRECISION U,CV
      DIMENSION CI(6,6),CIT(6,6),EPI(6,6),H(6),PH(6,6),S(6,6),
     1B(6,6),IM(3,3),IN(3,3),TS(3,3),TT(3,3),EP(6,6),EO(6,6),
     1AA(6,6)
   94 FORMAT (3E30.10)
   93 FORMAT (6E18.9)
   44 FORMAT (///)
  767 FORMAT(E15.8)
   91  FORMAT (10F7.5)
   92 FORMAT (3F15.10)
      READ (5,91) (ST(I),I=1,30)
      READ (5,92) (EO(K,K),K=1,6)
      WRITE (6,91) (ST(I),I=1,30)
      WRITE (6,44)
      N=3
   54 CONTINUE
      READ (5,92) (SS(J),J=1,3)
      CV=1.0/57.29577957
      PI=3.141593
      U=4686.8171*(3.6*2.4*3.6525)**2/(5.29*9.29)**3
      AM=(4./9.)**(1./3.)
      F=1./AM-1.
      TL=0.0
      AVN=3.*PI
      AI=-PI
      WRITE (6,93) PI,U,AM,F,AVN,AI
      WRITE (6,44)
      WRITE (6,94) (SS(J), J=1,3)
      WRITE (6,44)
      WRITE (6,93) (EO(K,K), K=1,6)
      WRITE (6,44)
   53 CALL TRUE (E,AI,F,EAC)
      CALL XTRP (EO,EAC)
      CALL NVRT (AA,EA)
      WRITE (6,93) ((AA(I,J), I=1,6),J=1,6)
      WRITE (6,44)
      CALL PERI (N,EP)
      WRITE (6,93) ((EP(K,L), K=1,6), L=1,6)
      DO 125 K=1,6
      EP(K,K)=SQRT(EP(K,K))
  125 WRITE(6,767) EP(K,K)
      WRITE (6,44)
      IF (N-2) 51,51,52
   51 N=3
   52 CONTINUE
      GO TO 54
      END
```

```
      SUBROUTINE VCTR(I,HMM)
      COMMON   U,CV,TL,BB,RME(30,3),VME(30,3),RBS(30,3),VBS(30,3),
     1IR45(3,3),RIL(3),VIL(3),R4(3),ST(30),EX(6,6),SS(3),E,AVN,EAP,F,PI,
     2AM
      DOUBLE PRECISION U,CV
      DIMENSION HMM(6,6),RHO(3),RHOD(3),TR13(3,3),RHOP(3),RHOPP(3),
     1CRHO(3),TR34(3,3),PWRA(3),PWRA1(3),PWRA2(3),PWRA3(3),
     1PWRL(3),PWRL3(3),VFK(3),C(3,3),RHOD1(3),RHO1(3),ERAT(3,3),
     1RP(3),VP(3),VKP(3)
      DIMENSION DUCK(200)
999   FORMAT(6E20.8)
997   FORMAT (3E20.8)
990   FORMAT (2E20.8)
      T=ST(I)
      XTL=0.0
      RIL(1)=1.0
      RIL(2)=0.0
      RIL(3)=0.0
      VIL(1)=0.0
      VIL(2)=5.228034445
      VIL(3)=0.0
      PWRA1(1)=1.0
      PWRA1(2)=0.0
      PWRA1(3)=0.0
      PWRL3(1)=0.0
      PWRL3(2)=DSQRT(U)
      PWRL3(3)=0.0
      CALL KEPLER (XTL,T,PWRA1,PWRL3,PWRA2,PWRA3)
      DO 15 II=1,3
      RBS(I,II)=PWRA2(II)
 15   VBS(I,II)=PWRA3(II)
      CALL KEPLER(XTL,T,RIL,VIL,RP,VP)
      CALL TRG(RP,VP,C)
      DO 11 K=1,3
      RHO(K)=RP(K)-RBS(I,K)
 11   RHOD(K)=VP(K)-VBS(I,K)
      RHOMAG =SQRT(RHO(1)**2&RHO(2)**2&RHO(3)**2)
      RHOMAG=(RHO(1)*RHOD(1)&RHO(2)*RHOD(2)&RHO(3)*RHOD(3))/RHOMAG
      DO 13 M=1,3
      RHOPP(M)=VBS(I,M)
 13   RHOP(M)=-RBS(I,M)
      CALL TR6(RHOPP,RHOP,TR13)
      CALL TRAFER(2,1,TR13,RHO,CRHO)
      EL=ASIN(CRHO(3)/RHOMAG)
      AZ=ASIN(CRHO(1)/RHOMAG/COS(EL))
      AZP=AZ
      IF (CRHO(2)) 20,21,22
 20   IF (CRHO(1)) 23,24,25
 23   AZ=PI-AZP
      GO TO 29
```

```
   24 AZ=PI
      GO TO 29
   25 AZ=PI&AZP
      GO TO 29
   21 IF (CRHO(1)) 26,27,28
   26 AZ=3.0*PI/2.0
      GO TO 29
   27 AZ=0.0
      GO TO 29
   28 AZ=PI/2.0
      GO TO 29
   22 AZ=AZP
   29 CONTINUE
      HMM(1,1)=COS(AZ)/RHOMAG/COS(EL)
      HMM(1,2)=-SIN(AZ)/RHOMAG/COS(EL)
      HMM(1,3)=0.0
      HMM(1,4)=0.0
      HMM(1,5)=0.0
      HMM(1,6)=0.0
      HMM(2,1)=-SIN(EL)*SIN(AZ)/RHOMAG
      HMM(2,2)=-SIN(EL)*COS(AZ)/RHOMAG
      HMM(2,3)=COS(EL)/RHOMAG
      HMM(2,4)=0.0
      HMM(2,5)=0.0
      HMM(2,6)=0.0
      VEK(1)=HMM(1,1)
      VEK(2)=HMM(1,2)
      VEK(3)=HMM(1,3)
      CALL TRAFER(1,2,TR13,VEK,VKP)
      CALL TRAFER(2,1,C,VKP,VEK)
      HMM(1,1)=VEK(1)
      HMM(1,2)=VEK(2)
      HMM(1,3)=VEK(3)
      VEK(1)=HMM(2,1)
      VEK(2)=HMM(2,2)
      VEK(3)=HMM(2,3)
      CALL TRAFER(1,2,TR13,VEK,VKP)
      CALL TRAFER(2,1,C,VKP,VEK)
      HMM(2,1)=VEK(2)
      HMM(2,2)=VEK(2)
      HMM(2,3)=VEK(3)
      SI=-(RHOD(1)*RHO(1)&RHOD(2)*RHO(2)&RHOD(3)*RHO(3))
      CALL TRAFER(2,1,C,RHOD,RHOD1)
      CALL TRAFER(2,1,C,RHO,RHO1)
      HMM(3,1)=RHOD1(1)/RHOMAG&SI*RHO1(1)/RHOMAG**3
      HMM(3,2)=RHOD1(2)/RHOMAG&SI*RHO1(2)/RHOMAG**3
      HMM(3,3)=RHOD1(3)/RHOMAG&SI*RHO1(3)/RHOMAG**3
      HMM(3,4)=RHO1(1)/RHOMAG
      HMM(3,5)=RHO1(2)/RHOMAG
      HMM(3,6)=RHO1(3)/RHOMAG
      RETURN
      END
```

```
      SUBROUTINE KEPLER(TIS,TSP,RIS,VIS,RS,VS)
      DIMENSION RIS(3),VIS(3),RS(3),VS(3)
      COMMON C,CV,TL,DB,RMF(30,3),VME(30,3),RBS(30,3),VBS(30,3),
     1TP45(3,3),RIL(3),VIL(3),R4(3),ST(30),EX(6,6),SS(3),E,AVN,EAP,F,PI,
     2AM
      DOUBLE PRECISION C,CV
      DOUBLE PRECISION RI(3),VI(3),R(3),V(3)
      DOUBLE PRECISION TI,TS,RDV,RIM,VIM,ENI,ALF,P,UDP,ARG,XN,CS,SR,EN,
     1II,RN,VM,A,B,ZN,ZM,TN,DTDX,X
      DOUBLE PRECISION TZ,C,S,G
      TI=TIS
      T=TSP
      DO 18 I=1,3
      RI(I)=RIS(I)
   18 VI(I)=VIS(I)
      UDP=C
      TS=T-TI
      RDV=RI(1)*VI(1)+RI(2)*VI(2)+RI(3)*VI(3)
      RIM=DSQRT(RI(1)**2+RI(2)**2+RI(3)**2)
      VIM=DSQRT(VI(1)**2+VI(2)**2+VI(3)**2)
      ENI=VIM**2/2.0-UDP/RIM
      ALF=(-2.0*ENI)/UDP
      K=0
      XN=.5
      P=2.0*3.141593*DSQRT(1.0/(UDP*(ALF**3)))
   17 IF (TS-P) 7,7,16
   16 TS=TS-P
      GO TO 17
    7 ARG=ALF*(XN**2)
      TZ=.5
      C=.5
      G=2.0
   21 G=G+2.0
      IF (DABS(TZ)-.0000000001) 19,19,20
   20 TZ=TZ*(-ARG)/(G*(G-1.0))
      C=C+TZ
      GO TO 21
   19 CR=C
      G=2.0
      TZ=1.0/6.0
      S=TZ
   24 G=G+2.0
      IF (DABS(TZ)-.0000000001) 22,22,23
   23 TZ=TZ*(-ARG)/(G*(G+1.0))
      S=S+TZ
      GO TO 24
   22 SR=S
      TN=(RDV/UDP)*(XN**2)*CR+((1.0-RIM*ALF)/DSQRT(UDP))*(XN**3)*SR-
     1RIM*XN/DSQRT(UDP)
      IF(DABS(TN-TS)-.00000001)1,1,2
    2 DTDX=(RDV/UDP)*(XN-ALF*(XN**3)*SR)+((1.0-RIM*ALF)/DSQRT(UDP))*
     1(XN**2)*CR+RIM/DSQRT(UDP)
```

```
      X=XN
      XN=X-(TN-TS)/DTDX
      IF(XN-36.0) 4,4,3
    3 XN=X6.5
    4 IF(XN) 5,6,6
    5 XN=X-.5
    6 K=K61
      IF (K-20) 7,7,8
    8 WRITE(6,11)
   11 FORMAT(15HERROR ITERATION,//)
      GO TO 12
    1 A=1.0-((XN**2)/RIM)*CR
      B=TN-((XN**3)/DSQRT(UDP))*SR
      DO 9 I=1,3
    9 R(I)=A*RI(I)6B*VI(I)
      RM=DSQRT(R(1)**26R(2)**26R(3)**2)
      ZM=(DSQRT(UDP)/(RM*RIM))*(ALF*(XN**3)*SR-XN)
      ZN=1.0-((XN**2)/RM)*CR
      DO 10 I=1,3
   10 V(I)=ZM*RI(I)6ZN*VI(I)
      VMSQ=V(1)**26V(2)**26V(3)**2
      EN=VMSQ/2.0-UDP/RM
      DO 25 I=1,3
      RS(I)=R(I)
   25 VS(I)=V(I)
      IF(DABS(EN-ENI)-.01) 12,12,13
   13 WRITE(6,14)
   14 FORMAT(12HERROR ENERGY,//)
   12 RETURN
      END


      SUBROUTINE TRADER(M,N,XMI,VIP,VECC)
      DOUBLE PRECISION C(3,3), VEC(3)
      DIMENSION XMI(3,3),VECC(3),VIP(3)
      DO 32 K=1,3
      DO 31 I=1,3
   31 C(K,I)=XMI(K,I)
   32 VEC(K)=VIP(K)
      IF(N-M) 71,72,73
   71 DO 74 I=1,3
   74 VECC(I) = VEC(1)*C(I,1)6VEC(2)*C(I,2)6VEC(3)*C(I,3)
      GO TO 77
   72 DO 75 I=1,3
   75 VECC(I)=VEC(I)
      GO TO 77
   73 DO 76 I=1,3
   76 VECC(I)=VEC(1)*C(1,I)6VEC(2)*C(2,I)6VEC(3)*C(3,I)
   77 RETURN
      END
```

```
      SUBROUTINE TR6(RP,VP,C)
      DIMENSION RP(3),VP(3),C(3,3)
      VMA=VP(1)**2&VP(2)**2&VP(3)**2
      IF (ABS(VMA-1.0)-.000001) 2,2,1
    2 VMAG=1.0
      GO TO 3
    1 VMAG=SQRT(VMA)
    3 C(2,1)=VP(1)/VMAG
      C(2,2)=VP(2)/VMAG
      C(2,3)=VP(3)/VMAG
      Z1=RP(2)*VP(3)-VP(2)*RP(3)
      Z2=RP(3)*VP(1)-VP(3)*RP(1)
      Z3= RP(1)*VP(2)-VP(1)*RP(2)
      ZMAG=SQRT(Z1**2&Z2**2&Z3**2)
      C(3,1)=Z1/ZMAG
      C(3,2)=Z2/ZMAG
      C(3,3)=Z3/ZMAG
      P1=VP(2)*Z3-VP(3)*Z2
      P2=VP(3)*Z1-VP(1)*Z3
      P3 =VP(1)*Z2-VP(2)*Z1
      PMAG=SQRT(P1**2&P2**2&P3**2)
      C(1,1)=P1/PMAG
      C(1,2)=P2/PMAG
      C(1,3)=P3/PMAG
      RETURN
      END



      SUBROUTINE XTRP(EC,EAC)
C     XTRP EXTRAPOLATES INITIAL COVARIANCE MATRIX(EC) FROM INITIAL
C     POINT(EAC/FAC) TO PERI-POINT
      COMMON   C,CV,TL,DB,RME(30,3),VME(30,3),RBS(30,3),VBS(30,3),
     1TR4B(3,3),RIL(3),VIL(3),R4(3),ST(30),BX(6,6),SS(3),E,AVN,EAP,F,PI,
     2AM
      DOUBLE PRECISION C,CV
      DIMENSION EC(6,6),ECI(6,6),CI(6,6),CIT(6,6),A(6,6),TM(3,3),TN(3,3)
     1,TS(3,3),TT(3,3)
      CALL MTRM(TM,E,EAC,EAP,AVN)
      CALL MTRN(TN,E,EAC,EAP,AVN)
      CALL MTRS(TS,E,EAC,EAP,AVN)
      CALL MTRT(TT,E,EAC,EAP,AVN)
      CALL CCLM (C,CI,CIT,TM,TN,TS,TT)
      CALL MVRT(ECI,EC)
      CALL MPY2(A,ECI,CI)
      CALL MPY2(EX,CIT,A)
      RETURN
      END
```

```
      SUBROUTINE TRUE(ECC,EMA,TA,E)
C     COMPUTE THE TRUE ANOMALY FOR ELLIPTIC OR HYPERBOLIC ORBIT
C     GIVEN THE MEAN ANOMALY AND ECCENTRICITY
      TOL= 1.0E-06
      CONV= 57.29577951
      IF(ABS(EMA)-TOL)80,90,90
   80 E=0.
      TA=0.
      GO TO 18
   90 IF(ECC-.001)20,30,30
   20 ROOT=1.
      GO TO 40
   30 ROOT= SQRT ( ABS ( (1.0 ECC)/(1.- ECC) ) )
   40 CONTINUE
    5 E=EMA
      DO 10 I=1,10
      DE=(EMA-(E-ECC*SIN (E)))/(1.-ECC*COS (E))
      E= E&DE
      IF( ABS (DE/E)- TOL) 15,15,10
   10 CONTINUE
   15 TA=2.0*ATAN(ROOT*SIN(E/2.)/COS(E/2.))
   18 RETURN
      END


      SUBROUTINE COOM(M,CI,CIT,TM,TN,TS,TT)
C     L=0 FOR CELESTIAL  L=1 FOR SAMPLES  M IS THE OPEN LOOP INDEX
      COMMON  L,CV,TL,DR,RME(30,3),VME(30,3),RRS(30,3),VRS(30,3),
     1TR45(3,3),RIL(3),VIL(3),R4(3),ST(30),EX(6,6),SS(3),E,AVN,EAP,F,PI,
     2AN
      DOUBLE PRECISION L,CV
      DIMENSION CI(6,6),CIT(6,6),TM(3,3),TN(3,3),TS(3,3),TT(3,3)
      IF (M) 2,2,1
    1 A=-DIRAVN*ST(M)
      CALL TRUE (E,A,F,EAC)
      CALL MTRM(TM,F,EAC,EAP,AVN)
      CALL MTRN(TN,E,EAC,EAP,AVN)
      CALL MTRS(TS,E,EAC,EAP,AVN)
      CALL MTRT(TT,E,EAC,EAP,AVN)
    2 DO 5 I=1,3
      DO 5 J=1,3
      CI(I,J)=TT(J,I)
       CI(I,J+3)=-TN(J,I)
      CI(I+3,J)=-TS(J,I)
      CI(I+3,J+3)=TM(J,I)
      CIT(I,J)=TT(I,J)
      CIT(I,J+3)=-TS(I,J)
      CIT(I+3,J)=-TN(I,J)
    5 CIT(I+3,J+3)=TM(I,J)
      RETURN
      END
```

```
      SUBROUTINE FIPI(A,EP)
      COMMON   L,CV,TL,PP,PME(30,3),VME(30,3),RBS(30,3),VBS(30,3),
     1TR4S(3,3),RIL(3),VIL(3),R4(3),ST(30),EX(6,6),SS(3),E,AVN,EAP,F,PI,
     2AM
      DOUBLE PRECISION L,CV
      DOUBLE PRECISION AA(6,6)
      DIMENSION CI(6,6),CII(6,6),FPI(6,6),H(6),HH(6,6),G(6,6),
     1P(6,6),TM(3,3),TN(3,3),TS(3,3),FP(6,6),FD(6,6),TT(3,3)
      DIMENSION FMM(6,6)
    61 FORMAT   (F30.15)
   993 FORMAT (6E18.9)
      DO 3 I=1,30
      MJ=6
      CALL CCIN(I,CI,CII,TM,TN,TS,TT)
      WRITE (6,61) ST(I)
      CALL VCIR (I,FMM)
      WRITE (6,993)((FMM(NJ,NJ),NJ=1,6),MJ=1,3)
      DO 5 J=1,N
      DO 7 KK=1,6
    7 P(KK)=FMM(J,KK)
      CALL MPY1 (EL,B)
      CALL MPY2(B,FP,CI)
      CALL MPY3 (C,CII,B)
      DO 8 K=1,6
      DO 9 L=K,6
      G(K,L)=G(K,L)/SS(J)
      AA(K,L)=G(K,L)+AA(K,L)
      IF (K-L) 2,3,2
    2 AA(L,K)=AA(K,L)
    9 CONTINUE
    8 CONTINUE
    5 CONTINUE
    3 CONTINUE
      CALL SUM (FPI,EX,AA)
      CALL NVRT (EP,FPI)
      DO 4 K=1,6
      DO 4 L=1,6
    4 AA(K,L)=0.0
      RETURN
      END

      SUBROUTINE NVRT(CC,CCC)
C     INVERSION OF 6X6 MATRIX
      COMMON   L,CV,TL,PP,PME(30,3),VME(30,3),RBS(30,3),VBS(30,3),
     1TR4S(3,3),RIL(3),VIL(3),R4(3),ST(30),EX(6,6),SS(3),E,AVN,EAP,F,PI,
     2AM
      DOUBLE PRECISION L,CV
      DOUBLE PRECISION C(6,12),S,DIV
      DIMENSION CC(6,6),CCC(6,6)
```

```
      DO 10 I=1,6,1
      DO 5 J=1,6,1
      G(I,J)=GGG(I,J)
    5 G(I,J66)=0.000000000
   10 G(I,I66)=1.000000000
      DO 30 I=1,6,1
      DO 14 J=I,6,1
      IF(DABS(G(I,I))-DABS(G(J,I)))11,14,14
   11 DO 12 K=1,6,1
      S=G(J,K)
      G(J,K)=G(I,K)
      G(I,K)=S
      S=G(J,K66)
      G(J,K66)=G(I,K66)
   12 G(I,K66)=S
   14 CONTINUE
      DIV=G(I,I)
      DO 15 J=1,6,1
      G(I,J)=G(I,J)/DIV
   15 G(I,J66)=G(I,J66)/DIV
      DO 30 J=1,6,1
      IF (I-J) 20,30,20
   20 DIV=G(J,I)
      DO 25 K=1,6,1
      G(J,K)=G(J,K)-G(I,K)*DIV
   25 G(J,K66)=G(J,K66)-G(I,K66)*DIV
   30 CONTINUE
      DO 35 I=1,6,1
      DO 35 J=1,6,1
   35 GG(I,J)=G(I,J66)
      RETURN
      END

      SUBROUTINE MTRM(C,ECC,EAC,EAD,ANVEL)
      DIMENSION C(3,3)
      E=ECC
      X=EAC
      Y=EAD
      Z=(Y-X)/2.
      L=(Y+X)/2.
      I=(2.*Z-ECC*SIN (Z)*COS (L))*(COS (Z)+ECC*COS (L ))-4.*SIN (Z)
      P=ANVEL
      SNX=SIN (X)
      SNY=SIN (Y)
      SNZ=SIN (Z)
      SNL=SIN (L)
      CSX=COS (X)
      CSY=COS (Y)
```

```
      CSZ=COS (Z)
      CSL=COS (L)
      ALPHA=SQRT (1.0-E**2)
      BETA=1.0-E*CSY
      DELTA=1.0-E*CSX
      PHI=1.0+E*CSX
      TZI=1.0+E*CSY
      GAMMA=    SQRT ((1.-E**2*CSX**2)*      (1.-E**2*CSY**2))
      C(1,1)=(      (PHI*BETA*((2.*SNZ*BETA)/DELTA**2)*((1.-E**2)
     1*SNZ-(DELTA*E*SNX*CSZ)))/GAMMA
      C(1,2)=(      ((2.*ALPHA*BETA)/DELTA**2)*SNZ*(CSZ-E*CSL))/GAMMA
      C(1,3)=0.0
      C(2,1)=(((      2.*ALPHA)/(DELTA**2)*((-TZI)*(3.*Z-E*SNZ*CSL)&2.
     1*SNZ*(E*CSL&CSZ*(1.0+E*CSX-E**2*CSX**2))))/GAMMA
      C(2,2)=      (((DELTA*TZI*((2.0/DELTA**2)*((-TZI)*E*SNX*(3.*Z-E*SNZ
     1*CSL)&2.0*SNZ*(2.0*E*SNL-(1.0+E**2)*SNZ))) )/GAMMA
      C(2,3)=0.0
      C(3,1)=0.0
      C(3,2)=0.0
      C(3,3)=1.-((2.*SNZ**2)/DELTA)
      RETURN
      END

      SUBROUTINE MTRX(E,ECC,EAC,EAC,ANVEL)
      DIMENSION F(3,3)
      E=ECC
      BETA=2./ANVEL
      X=EAC
      Y=EAC
      Z=(Y-X)/2.
      L=(Y+X)/2.
      T=(3.*Z-ECC*SIN (Z)*COS (L))*(COS (Z)+ECC*COS (L ))-4.*SIN (Z)
      SNX=SIN (X)
      SNY=SIN (Y)
      SNZ=SIN (Z)
      SNL=SIN (L)
      CSX=COS (X)
      CSY=COS (Y)
      CSZ=COS (Z)
      CSL=COS (L)
      ALPHA=SQRT (1.0-E**2)
      GAMMA=BETA/(SQRT (1.-E**2*CSX**2)*SQRT (1.-E**2*CSY**2))
      PHI=1.0+E*CSX
      TZI=1.0+E*CSY
      F(1,1)=GAMMA*PHI*TZI*SNZ*(CSZ+E*CSL)
      F(1,2)=GAMMA*2.0*ALPHA*TZI*SNZ**2
      F(1,3)=0.0
      F(2,1)=-(GAMMA*2.*ALPHA*PHI*SNZ**2)
```

```
      F(2,2)=GAMMA*(4.*SNZ*(CSZ&E*CSL)-(1.&E*CSX)*(1.&E*CSY)*(3.*Z-
     1E*SNZ*CSL))
      F(2,3)=0.0
      F(3,1)=0.0
      F(3,2)=0.0
      F(3,3)=BETA*SNZ*(CSZ-E*CSL)
      RETURN
      END


      SUBROUTINE MTRS(S,ECC,EAC,LAT,ANVEL)
      DIMENSION S(3,3)
      E=ECC
      X=EAC
      Y=EAC
      Z=(Y-X)/2.
      L=(Y&X)/2.
      I=(3.*Z-ECC*SIN (Z)*COS (L))*(COS (Z)&ECC*COS (L ))-4.*SIN (Z)
      B=ANVEL
      SNX=SIN (X)
      SNY=SIN (Y)
      SNZ=SIN (Z)
      SNL=SIN (L)
      CSX=COS (X)
      CSY=COS (Y)
      CSZ=COS (Z)
      CSL=COS (L)
      ALPHA=1.0-E**2
      BETA=1.0-E*CSX
      DELTA=1.0-E*CSY
      GAMMA=(2.0*B)/(BETA**2*DELTA**2*SQRT (1.0-E**2*CSX**2)*SQRT (1.0-E
     1**2*CSY**2))
      S(1,1)=GAMMA*(ALPHA*(3.0*Z-2.0)*E*SNZ*CSL)-(BETA*DELTA*E**2*SNX*
     1SNY&ALPHA*(1.0&BETA*E*CSX&BETA*E*CSY*DELTA))*SNZ*CSZ)
      S(1,2)=GAMMA*SQRT (ALPHA)*(2.0*E*SNX*(Z-E*SNZ*CSL)&SNZ**2*(ALPHA&E
     1*CSY*DELTA)-E**2*SNZ*SNL*(2.0*BETA*CSZ*CSL&CSY*DELTA))
      S(1,3)=0.0
      S(2,1)=GAMMA*SQRT (ALPHA)*(2.0*E*SNY*(Z-E*SNZ*CSL)-SNZ**2*(ALPHA
     1&E* CSX*BETA)-E**2*SNZ*SNL*(2.0*DELTA*CSZ*CSL&CSX*BETA))
      S(2,2)=GAMMA*(E**2*SNX*SNY*(3.0*Z-4.0*E*SNZ*CSL&E**2*SNZ*CSZ*(CSL*
     1*2-SNL**2))-ALPHA*SNZ*(CSZ*(1.0&E**2)-2.0*E*CSL))
      S(2,3)=0.0
      S(3,1)=0.0
      S(3,2)=0.0
      S(3,3)=-(2.*B*((SNZ*CSZ)/(BETA*DELTA)))
      RETURN
      END
```

```
      SUBROUTINE MTRT(T,ECC,EAC,EAP,ANVEL)
      DIMENSION T(3,3)
      E=ECC
      X=EAC
      Y=EAP
      Z=(Y-X)/2.
      L=(Y&X)/2.
      B=ANVEL
      SNX=SIN (X)
      SNY=SIN (Y)
      SNZ=SIN (Z)
      SNL=SIN (L)
      CSX=COS (X)
      CSY=COS (Y)
      CSZ=COS (Z)
      CSL=COS (L)
      ALPHA=1.0-E**2
      BETA=1.0-E*CSX
      DELTA=1.0-E*CSY
      PHI=1.0&E*CSX
      TZI=1.0&E*CSY
      GAMMA=    SQRT ((1.-E**2*CSX**2)*      (1.-E**2*CSY**2))
      T(1,1)=      (((TZI*BETA&((2.*SNZ*BETA)/DELTA**2)*(ALPHA*SNZ&DELTA
     1*E*SNY*CSZ)))/GAMMA
      T(1,2)=(((      2.*SQRT (ALPHA))/DELTA**2)*(PHI*(3.*Z-E*SNZ*CSL)
     1-2.0*SNZ*(E*CSL&CSZ*(TZI-E**2*(SY**2))))/GAMMA
      T(1,3)=0.0
      T(2,1)=-((      (((2.*SQRT (ALPHA)*BETA)/DELTA**2)*SNZ*(CSZ-E*CSL
     1)))))/GAMMA
      T(2,2)=(      (DELTA*PHI&(2.0/DELTA**2)*(PHI*E*SNY*(3.0*Z-E*SNZ
     1*CSL)-2.0*SNZ*(2.0*E*SNL&SNZ*(1.0&E**2)))))/GAMMA
      T(2,3)=0.0
      T(3,1)=0.0
      T(3,2)=0.0
      T(3,3)=1.-((2.*SNZ**2)/DELTA)
      RETURN
      END
```

```
      SUBROUTINE MPY1(FF,F)
      COMMON   L,CV,IL,ZB,RME(30,3),VME(30,3),RBS(30,3),VBS(30,3),
     1TR45(3,3),RIL(3),VIL(3),R4(3),ST(30),FX(6,6),SS(3),F,AVN,FAP,F,PI,
     2AM
      DOUBLE PRECISION L,CV
      DOUBLE PRECISION A(6)
      DIMENSION F(6),FF(6,6)
      DO 1 I=1,6
    1 A(I)=F(I)
      DO 2 I=1,6
      DO 2 J=1,6
      FF(I,J)=A(I)*A(J)
       IF(I-J) 2,3,2
    2 FF(J,I)=FF(I,J)
    3 CONTINUE
      RETURN
      END



      SUBROUTINE MPY2(XX,XY,XZ)
      COMMON   L,CV,IL,ZB,RME(30,3),VME(30,3),RBS(30,3),VBS(30,3),
     1TR45(3,3),RIL(3),VIL(3),R4(3),ST(30),FX(6,6),SS(3),F,AVN,FAP,F,PI,
     2AM
      DOUBLE PRECISION L,CV
C     XY TIMES XZ
      DOUBLE PRECISION A(6,6),B(6,6),C(6,6)
      DIMENSION XX(6,6),XY(6,6),XZ(6,6)
      DO 2 J=1,6
      DO 2 K=1,6
      A(J,K)=XY(J,K)
    2 B(J,K)=XZ(J,K)
      DO 1 J=1,6
      DO 1 K=1,6
      C(J,K)=0.
      DO 1 L=1,6
    1 C(J,K)=C(J,K)+A(J,L)*B(L,K)
      DO 3 J=1,6
      DO 3 K=1,6
    3 XX(J,K)=C(J,K)
      RETURN
      END
```

```
      SUBROUTINE MPY3(XX,XY,XZ)
C     XY TIMES XZ, XX IS SYMMETRIC
      COMMON  L,CV,IL,PB,RME(30,3),VME(30,3),RBS(30,3),VBS(30,3),
     1TR45(3,3),RIL(3),VIL(3),R4(3),ST(30),EX(6,6),SS(3),L,AVN,EAP,F,PI,
     2AM
      DOUBLE PRECISION L,CV
      DOUBLE PRECISION A(6,6),B(6,6),C(6,6)
      DIMENSION XX(6,6),XY(6,6),XZ(6,6)
      DO 4 J=1,6
      DO 4 K=1,6
      A(J,K)=XY(J,K)
    4 B(J,K)=XZ(J,K)
      DO 3 J=1,6,1
      DO 3 K=J,6,1
      C(J,K)=0.
      DO 3 L=1,6,1
      C(J,K)=C(J,K)+A(J,L)*B(L,K)
      IF (L-6) 3,1,1
    1 IF (J-K) 2,3,2
    2 C(K,J)=C(J,K)
    3 CONTINUE
      DO 5 J=1,6
      DO 5 K=1,6
    5 XX(J,K)=C(J,K)
      RETURN
      END
```

```
      SUBROUTINE SUM(ZX,ZY,C)
      ZY(6,6), ZX IS SYMMETRIC
      DOUBLE PRECISION A(6,6),B(6,6),C(6,6)
      DIMENSION ZY(6,6),ZX(6,6)
      DO 3 I=1,6
      DO 3 J=1,6
    3 B(I,J)=ZY(I,J)
      DO 4 J=1,6,1
      DO 4 K=J,6,1
      A(J,K)=B(J,K)+C(J,K)
      IF (J-K) 1,2,1
    1 A(K,J)=A(J,K)
    2 CONTINUE
      DO 4 I=1,6
      DO 4 J=1,6
    4 ZX(I,J)=A(I,J)
      RETURN
      END
```

PROGRAM INPUT DATA

MEASUREMENT TIMES IN YEARS PAST INJECTION

.026099.054757.098563.175222.219028.284736.295688.317591.350445.383299
.415202.416153.449008.481862.503765.514716.580424.602327.624230.635181
.700800.744695.777550.799452.821355.854209.876112.898015.941821.963723

INJECTION ERROR COVARIANCE MATRIX(DIAGONAL ELEMENTS)

.107010000E-06.107010000E-06.107010000E-06
.153300000E-02.290270000E-03.153300000E-02

MEASUREMENT ERROR COVARIANCE MATRIX(DIAGONAL ELEMENTS) FOR VARYING QUALITIES OF RANGE RATE

.304000000E-05.304000000E-05.177400000E-02
.304000000E-05.304000000E-05.399000000E-02
.304000000E-05.304000000E-05.444000000E-03
.304000000E-05.304000000E-05.160000000E-03
.304000000E-05.304000000E-05.400000000E-04
.304000000E-05.304000000E-05.444000000E-05
.304000000E-05.304000000E-05.400000000E-06
.304000000E-05.304000000E-05.160000000E-07
.304000000E-05.304000000E-05.400000000E-08
.304000000E-05.304000000E-05.160000000E-09
.304000000E-05.304000000E-05.400000000E-10
.304000000E-03.304000000E-03.160000000E-07

A.5 Listing of the Geometrically Exact Program.

```
GO          DOFRER  EAL

            COMMON   U,CV,TL,BB,RME(30,3),VME(30,3),RBS(30,3),VBS(30,3),
           1TR45(3,3),RIL(3),VIL(3),R4(3),ST(30),EX(6,6),SS(3),E,AVN,EAP,F,PI,
           2AM
            DOUBLE PRECISION U,CV
            DOUBLE PRECISION RMEE(30,3),VMEE(30,3),RBSE(30,3),VBSE(30,3),CO,
           1SN,EBAR,CON,RG
            DIMENSION HMM(6,6),VBI(3),RBI(3),RDS(3),VDS(3)
            DIMENSION CI(6,6),CIT(6,6),EPI(6,6),H(6),HH(6,6),S(6,6),
           1        TM(3,3),TN(3,3),TS(3,3),TT(3,3),EP(6,6),EO(6,6),
           1AA(6,6)
         94 FORMAT (3E30.10)
         93 FORMAT (6E18.9)
         44 FORMAT (///)
         91  FORMAT (10F7.5)
         92 FORMAT (3E15.10)
        111 FORMAT(3E15.8)
        767 FORMAT(E15.8)
            READ (5,91) (ST(I),I=1,30)
            READ (5,92) (EO(K,K),K=1,6)
            WRITE (6,91) (ST(I),I=1,30)
            WRITE (6,44)
            DO 112 M=1,30
            READ(5,111) (RBSE(M,J),J=1,3)
            READ(5,111) (VBSE(M,J),J=1,3)
            READ(5,111) (RMEE(M,J),J=1,3)
        112 READ(5,111) (VMEE(M,J),J=1,3)
            CV=1.0/57.29577957
            EBAR=23.4457587*CV
            CO=DCOS(EBAR)
            SN=DSIN(EBAR)
            CON=149599000/6378.3255
            DO 101 I=1,30
            RME(I,1)=RMEE(I,1)/CON
            RME(I,2)=(RMEE(I,2)*CO-RMEE(I,3)*SN)/CON
            RME(I,3)=(RMEE(I,2)*SN&RMEE(I,3)*CO)/CON
            VME(I,1)=VMEE(I,1)*365.25/CON
            VME(I,2)=(VMEE(I,2)*CO-VMEE(I,3)*SN)*365.25/CON
            VME(I,3)=(VMEE(I,2)*SN&VMEE(I,3)*CO)*365.25/CON
            RBS(I,1)=RBSE(I,1)
            RBS(I,2)=RBSE(I,2)*CO-RBSE(I,3)*SN
            RBS(I,3)=RBSE(I,2)*SN&RBSE(I,3)*CO
            VBS(I,1)=VBSE(I,1)*365.25
            VBS(I,2)=(VBSE(I,2)*CO-VBSE(I,3)*SN)*365.25
        101 VBS(I,3)=(VBSE(I,2)*SN&VBSE(I,3)*CO)*365.25
            N=3
         54 CONTINUE
```

```
      READ (5,92) (SS(J),J=1,3)
      PI=3.141593
      U=4686.3171*(3.6*2.4*3.6525)**2/(5.28*9.22)**3
      VIL(1)=4.593304522
      VIL(2)=2.290636416
      VIL(3)=.9934196138
      A=28.84*CV
      B=263.75*CV
      TI=6046.0
      RIL(1)=.4775747926
      RIL(2)=-.8066642391
      RIL(3)=-.3495465269
      RG=0.0000042603278
      R4(1)=COS(A)*COS(B)*RG
      R4(2)=COS(A)*SIN(B)*RG
      R4(3)=SIN(A)*RG
      CALL TR3(A,B,TR45)
      AM=(4./3.)**(1./3.)
      E=1./AM-1.
      AVN=3.*PI
      AI=-PI
      WRITE (6,93) PI,U,AM,E,AVN,AI
      WRITE (6,44)
      WRITE (6,94) (SS(J), J=1,3)
      WRITE (6,44)
      WRITE (6,93) (EC(K,K), K=1,6)
      WRITE (6,44)
   58 CALL TRUE (E,AI,F,EAC)
      CALL KEP2 (EO,EAC)
      CALL NVRT (AA,FX)
      WRITE (6,93) ((AA(I,J), I=1,6),J=1,6)
      WRITE (6,44)
      CALL PERI (N,EP)
      WRITE (6,93) ((EP(K,L), K=1,6), L=1,6)
      WRITE (6,44)
      DO 125 K=1,6
      EP(K,K)=SQRT(EP(K,K))
  125 WRITE(6,767) EP(K,K)
      IF (N-2) 51,51,52
   51 N=3
   52 CONTINUE
      GO TO 54
      END
```

```
      SUBROUTINE VCTR(I,HMM)
      COMMON   U,CV,TL,34,RME(30,3),VME(30,3),RPS(30,3),VPS(30,3),
     1TR45(3,3),RIL(3),VIL(3),R4(3),ST(30),EX(6,6),SS(3),E,AVM,EAP,F,PI,
     2AM
      DOUBLE PRECISION U,CV
      DIMENSION HMM(6,6),RHO(3),RHOD(3),TR13(3,3),RHOP(3),RHOPP(3),
     1QRHO(3),TR34(3,3),PWRA(3),PWRA1(3),PWRA2(3),PWRA3(3),
     1PWRL(3),PWRL3(3),VIK(3),C(3,3),RHOD1(3),RHO1(3),TRAT(3,3),
     1RP(3),VP(3),VKP(3)
 225 FORMAT (5E15.8)
 247 FORMAT(3E15.8)
 248 FORMAT(E15.8)
 249 FORMAT(2E15.8)
      T=ST(I)
      PI=1.0/32.3915
      XJD=TL*365.25
      XJC=TL/36525.0+1/100.0
      XJI=FLOAT(IFIX(XJD))
      XJS=3600.0*24.0*(XJC-XJI)
      CALL TR1(XJC,XJL,TR13)
      CALL TR2(-1,XJI,XJS,TR34)
      CALL TR2(2,XJI,XJS,TRAT)
      XTL=0.0
      CALL KEPLER(XTL,T,RIL,VIL,RP,VP)
      CALL TR3(RP,VP,C)
      CALL TRAFR(4,3,TR34,R4,RHO1)
      CALL TRAFR2(1,3,TR13,RHO1,RHOP)
      CALL TRAFR(4,3,TRAT,R4,RHOD1)
      CALL TRAFR(1,3,TR13,RHOD1,RHOD)
      DO 11 K=1,3
      RHO(K)=RP(K)*2.0*VME(I,K)-RPS(I,K)-RHOP(K)
      RHOP(K)=VP(K)*2.0*VME(I,K)-VPS(I,K)
   11 RHOPP(K)=VP(K)*2.0*VME(I,K)-VPS(I,K)-QRHO(K)
      RHOMAG=SQRT(RHO(1)**2+RHO(2)**2+RHO(3)**2)
      RHOPMAG=(RHO(1)*RHOP(1)+RHO(2)*RHOP(2)+RHO(3)*RHOP(3))/RHOMAG
      RHOPPMAG=(RHO(1)*RHOPP(1)+RHOP(2)*RHOPP(2)+RHOP(3)*RHOPP(3))/RHOMAG
      CALL TRAFR(3,1,TR13,RHO,RHOP)
      CALL TRAFR(3,4,TR34,RHOP,RHOPP)
      CALL TRAFR(4,3,TR43,RHOPP,QRHO)
      EL=ASIN(-QRHO(3)/RHOMAG)
      AZ=ATAN2(QRHO(2)/(RHOMAG*COS(EL)))
      AZP=AZ
      IF (QRHO(1)) 20,21,22
   22 IF (QRHO(2)) 23,24,25
   23 AZ=PI-AZP
      GO TO 29
   24 AZ=PI
      GO TO 29
```

```
25 AZ=PI&AZP
   GO TO 29
21 IF (QRHO(2)) 26,27,28
26 AZ=3.0*PI/2.0
   GO TO 29
27 AZ=0.0
   GO TO 29
28 AZ=PI/2.0
   GO TO 29
22 AZ=AZP
29 CONTINUE
   HMM(1,1)=-SIN(AZ)/RHOMAG/COS(EL)
   HMM(1,2)=COS(AZ)/RHOMAG/COS(EL)
   HMM(1,3)=0.0
   HMM(1,4)=0.0
   HMM(1,5)=0.0
   HMM(1,6)=0.0
   HMM(2,1)=-SIN(EL)*COS(AZ)/RHOMAG
   HMM(2,2)=-SIN(EL)*SIN(AZ)/RHOMAG
   HMM(2,3)=-COS(EL)/RHOMAG
   HMM(2,4)=0.0
   HMM(2,5)=0.0
   HMM(2,6)=0.0
   DO 30 K=1,2
   VEK(1)=HMM(K,1)
   VEK(2)=HMM(K,2)
   VEK(3)=HMM(K,3)
   CALL TRAFER(5,4,TR45,VEK ,PWRA1)
   CALL TRAFER(4,3,TR34,PWRA1,PWRA2)
   CALL TRAFER(1,3,TR13,PWRA2,PWRA3)
   CALL TRAFER(2,1,C,PWRA3,VKP)
   HMM(K,1)=VKP(1)
   HMM(K,2)=VKP(2)
30 HMM(K,3)=VKP(3)
   SI=-(RHOD(1)*RHO(1)&RHOD(2)*RHO(2)&RHOD(3)*RHO(3))
   CALL TRAFER(2,1,C,RHOD,RHOD1)
   CALL TRAFER(2,1,C,RHO,RHO1)
   DO 31 IK=1,3
   HMM(3,IK)=RHOD1(IK)/RHOMAG&SI*RHO1(IK)/RHOMAG**3
   IP=IK&3
31 HMM(3,IP)=RHO1(IK)/RHOMAG
   RETURN
   END
```

```
      SUBROUTINE TR1(T,TC,C)
      COMMON   L,CV,TL,EE,RME(3C,3),VME(3C,3),RBS(3C,3),VBS(3C,3),XMC,
     1TR45(3,3),RIL(3),VIL(3),R4(3),ST(3C)
      DOUBLE PRECISION L,CV
      DIMENSION C(3,3), A(3,3), B(3,3), C(3)
      DOUBLE PRECISION ADP(3,3), BDP(3,3)
      A(1,1)=1.C-C.CCC29697*(T**2.)-C.CCCCCC13*(T**3.)
      A(1,2)=-C.C2234SEE*T-C.CCCCC676*(T**2.)EC.CCCCC221*(T**3.)
      A(2,1)=-A(1,2)
      A(1,3)=-C.CC971711*TEC.CCCCC2C7*(T**2.)EC.CCCCCC9E*(T**3.)
      A(3,1)=-A(1,3)
      A(2,2)=1.C-C.CCC24976*(T**2.)-C.CCCCCC15*(T**3.)
      A(2,3)=-C.CCC1CE59*(T**2.)-C.CCCCCCC3*(T**3.)
      A(3,2)=A(2,3)
      A(3,3)=1.C-C.CCCC4721*(T**2.)EC.CCCCCCC2*(T**3.)
      Y=C.CCC1
      CM=CV*(12.1127SC2-C.C52953222*TCE2C.795*Y*TE2C.F1*Y*(T**2.)EC.C2*
     1Y*(T**3.))
      SL=CV*(E4.37545167813.17E3E52CE*TC-11.31575*Y*T-11.3C15*Y*(T**2.)
     1EC.C19*Y*(T**3.))
      CP=CV*(2CE.E439E77EC.1114C4CFC3*TC-C.C1C334*T-C.C1C343*(T**2.)-
     1C.12*Y*(T**3.))
      CL=CV*(2EC.CE121CC9EC.9E5E473354*TCE3.C3*Y*TE3.C3*Y*(T**2.))
      C=CV*(2E2.CECC53C2EEC.47CEE4*Y*TCE4.5525*Y*TE4.575*Y*(T**2.)EC.C3*Y
     1*(T**3.))
      DSI=-C.5658*Y*SIN(2.C*SL)-C.C95C*Y*SIN(2.C*SL-CM)-C.C725*Y*SIN(3.C
     1*SL-CP)EC.C217*Y*SIN(SLECP)EC.C1E1*Y*SIN(SL-CPECM)EC.C158*Y*SIN(SL
     2-CP-CM)-C.C144*Y*SIN(3.C*SLECP-2.C*CL)-C.C122*Y*SIN(3.C*SL-CP-CM)E
     3C.1E75*Y*SIN(SL-CP)EC.CC78*Y*SIN(2.C*SL-2.C*CP)EC.C414*Y*SIN(SLECP
     4-2.C*CL)EC.C167*Y*SIN(2.C*SL-2.C*CL)-C.CCP5*Y*SIN(4.C*SL-2.C*CL)
      DELSI=-(47.E527EC.C482*T)*Y*SIN(CM)EC.5ECC*Y*SIN(2.C*CM)-3.5361*Y*
     1SIN(2.C*CL)-C.1378*Y*SIN(3.C*CL-C)EC.C554*Y*SIN(CLEC)EC.C344*Y*
     2SIN(2.C*CL-CM)EC.C125*Y*SIN(2.C*CP-CM)EC.35CC*Y*SIN(CL-C)E
     3C.C125*Y*SIN(2.C*CL-2.C*CP)
      DF= (C.2456*CCS(2.C*SL)EC.C5C8*CCS(2.C*SL-CM)EC.C365*
     1CCS(3.C*SL-CP)-C.C139*CCS(SLECP)-C.CCE6*CCS(SL-CPECM)EC.CEE3*
     2CCS(SL-CP-CM)EC.CC61*CCS(3.C*SLECP-2.C*CL)EC.CC64*
     3CCS(3.C*SL-CP-CM))*Y
      DELF=(25.5E44*CCS(CM)-C.2511*CCS(2.C*CM)E1.533E*CCS(2.C*CL)EC.CEEE
     1*CCS(3.C*CL-C)-C.C25E*CCS(CLEC)-C.C1E3*CCS(2.C*CL-CM)-C.CC67*
     2CCS(2.C*CP-CM))*Y
      DELTAE=(DELEEDE)*CV
      DELTSI=(DELSIEDSI)*CV
      EER=(23.4457587-C.C13C94C4*T-C.CCEE*Y*(T**2.)EC.CC5C*Y*(T**3.))*CV
      B(1,1)=1.C
      B(2,2)=1.C
      B(3,3)=1.C
      B(1,2)=-DELTSI*CCS(EER)
      B(2,1)=-B(1,2)
      EE=B(2,1)
      B(1,3)=-DELTSI*SIN(EER)
      B(3,1)=-B(1,3)
      B(2,3)=-DELTAE
      B(3,2)=-B(2,3)
```

```
      DO 1 I=1,3
      DO 1 M=1,3
      DO 2 N=1,3
      ADF(N,M)=A(N,M)
      BDF(I,N)=B(I,N)
    2 C(N)=BDF(I,N)*ALF(N,M)
    1 D(I,M)=C(1)*C(2)*C(3)
      RETURN
      END


      SUBROUTINE TR2(N,TC,TS,D)
      COMMON   L,CV,IL,EE,RME(3C,3),VME(3C,3),RBS(3C,3),VBS(3C,3),XMC,
     1TR45(3,3),RIL(3),VIL(3),R4(3),ST(3C)
      DOUBLE PRECISION L,CV
      DIMENSION D(3,3)
      P=C.CC417EC7417/(1.CE5.21*TE*(.CCCCCCCCCCCC1))
      HAM=1CC.C755426CE.9E5E4734EC*TE*2.9C15*(.CCCCCCCCCCCC1)*
     1(TE**2)*EP*TS
   15 IF (36C.C-HAM) 8,9,9
    8 HAM=HAM-36C.C
      GO TO 15
    9 HAM=CV*HAM
      HA=HAM+EE
      IF (N) 1C,11,12
   1C D(1,1)=COS(HA)
      D(1,2)=-SIN(HA)
      D(1,3)=C.C
      D(2,1)=-D(1,2)
      D(2,2)=D(1,1)
      D(2,3)=C.C
      D(3,1)=C.C
      D(3,2)=C.C
      D(3,3)=1.C
      GO TO 14
   11 Z=9E.C
      WRITE (6,13) Z
   13 FORMAT   (F15.1C)
      GO TO 14
   12 W=W*CV*36CC.C*3E5.25*24.C
      D(1,1)=-W*SIN(HA)
      D(1,2)=-W*COS(HA)
      D(1,3)=C.C
      D(2,1)=W*COS(HA)
      D(2,2)=-W*SIN(HA)
      D(2,3)=C.C
      D(3,1)=C.C
      D(3,2)=C.C
      D(3,3)=C.C
   14 RETURN
      END
```

```
      SUBROUTINE TR3(PHI,GLCN,L)
      COMMON   L,CV,TL,EE,RME(3C,3),VME(3C,3),RPS(3C,3),VPS(3C,3),XMC,
     1TR45(3,3),RIL(3),VIL(3),R4(3),ST(3C)
      DOUBLE PRECISION L,CV
      DIMENSION E(3,3)
      E(1,1)=-SIN(PHI)*COS(GLCN)
      E(1,2)=-SIN(GLCN)
      E(1,3)=-COS(PHI)*COS(GLCN)
      E(2,1)=-SIN(PHI)*SIN(GLCN)
      E(2,2)=COS(GLCN)
      E(2,3)=-COS(PHI)*SIN(GLCN)
      E(3,1)=COS(PHI)
      E(3,2)=C.C
      E(3,3)=-SIN(PHI)
      RETURN
      END
```

REFERENCES

1. Baker, R.H., and others, Study of a Small Solar Probe, Part II, Center for Space Research, M.I.T., Cambridge, Mass., 1965.

2. Battin, Richard H., Astronautical Guidance, McGraw-Hill, Inc., New York, 1964.

3. Bryson, A.E., and Ho, Y., Optimal Programming, Estimation, and Control, to be published by Blaisdell.

4. Carr, Russell E., and Hudson, R. Henry, Tracking and Orbit Determination Program of the Jet Propulsion Laboratory, Tech. Report No. 32-7, Jet Propulsion Laboratory, Calif. Institute of Technology, Pasadena, Calif., 1960.

5. Deutsch, Ralph, Orbital Dynamics of Space Vehicles, Prentice-Hall, Englewood Cliffs, N.J., 1963.

6. Draper, Charles S., Wrigley, Walter, and Hovorka, John, Inertial Guidance, The Macmillan Company, New York, 1960.

7. Escobal, Pedro Ramon, Methods of Orbit Determination, John Wiley and Sons, Inc., N.Y. |London| Sydney, 1965.

8. Explanatory Supplement to the Ephemeris, Her Majesty's Stationery Office, London, 1961.

9. Harrington, John V., Study of a Small Solar Probe, Part I, Center for Space Research, M.I.T., Cambridge, Mass., 1965.

10. Holdridge, D.B., Space Trajectories Program for the IBM 7090 Computer, Tech. Report No. 32-223, Jet Propulsion Laboratory, Calif. Institute of Technology, Pasadena Calif., 1962.

11. Kopal, Zdeněk (ed.), Physics and Astronomy of the Moon, Academic Press, New York, 1962.

12. Ling-Temco-Vought, Inc., Astronautics Division, Feasibility and Parametric Design Study of an Unguided Solid Fuel Rocket Vehicle with Solar Orbit Capabilities, Dallas, 1965.

13. Madl, Dennis O., Sunblazer State Determination Investigation, Center for Space Research, M.I.T., Cambridge, Mass., 1966.

14. Peabody, P.R., Scott, J.F., and Orozco, E.G., JPL Ephemeris Tapes E9510, E9511, and E9512, Tech. Memorandum No. 33-167, Jet Propulsion Laboratory, Calif. Institute of Technology, Pasadena, Calif., 1964.

15. Peabody, P.R., Scott, J.F., and Orozco, E.G., User's Description of JPL Ephemeris Tapes, Tech. Report No. 32-580, Jet Propulsion Laboratory, Calif. Institute of Technology, Pasadena, Calif., 1964.

16. Potter, James E., and Stern, Robert G., Statistical Filtering of Space Navigation Measurements, RE-3, Experimental Astronomy Laboratory, M.I.T., Cambridge, Mass., 1963.

17. The American Ephemeris and Nautical Almanac for the Year 1966, U.S. Government Printing Office, Washington, 1964.

18. Private discussion with Dr. Jesse James, Center for Space Research, M.I.T., Cambridge, Mass.